Research
A SCIENCE PARTNER JOURNAL

REVIEW ARTICLE

The Heterogeneity and Function of Stromal Cells in the Tumor Microenvironment

Xuehai Wang[1†], Songlin Li[2†], Yang Xue[1†], Xiao Liang[3], Xuelei Ma[3*], Kun Zhang[1*], and Ying Wang[2*]

[1]Department of Thoracic Surgery, Sichuan Academy of Medical Sciences and Sichuan Provincial People's Hospital, University of Electronic Science and Technology of China, Chengdu, Sichuan Province, China. [2]Department of Oncology, Sichuan Academy of Medical Sciences and Sichuan Provincial People's Hospital, University of Electronic Science and Technology of China, Chengdu, Sichuan Province, China. [3]Department of Biotherapy, State Key Laboratory of Biotherapy, West China Hospital, Sichuan University, Chengdu, Sichuan Province, China.

*Address correspondence to: drmaxuelei@gmail.com (X.M.); ldw617@163.com (K.Z.); 17380405630@163.com (Y.W.)
†These authors contributed equally to this work.

Citation: Wang X, Li S, Xue Y, Liang X, Ma X, Zhang K, Wang Y. The Heterogeneity and Function of Stromal Cells in the Tumor Microenvironment. *Research* 2026;9:Article 1183. https://doi.org/10.34133/research.1183

Submitted 29 December 2025
Revised 5 February 2026
Accepted 10 February 2026
Published 9 March 2026

Copyright © 2026 Xuehai Wang et al. Exclusive licensee Science and Technology Review Publishing House. No claim to original U.S. Government Works. Distributed under a Creative Commons Attribution License (CC BY 4.0).

The tumor microenvironment is a central determinant of cancer progression, metastatic spread, and therapeutic resistance. Once considered passive scaffolds, stromal cells are now recognized as heterogeneous, active regulators of tumor behavior. Recent single-cell and spatial multiomics studies have resolved functionally distinct stromal subtypes, each defined by characteristic molecular programs and spatial niches, with specialized roles in extracellular matrix remodeling, immune evasion, and angiogenesis. This review synthesizes evidence for bidirectional stromal–tumor cross-talk in which cytokine networks (e.g., transforming growth factor-beta, interleukin-6, and C-X-C motif chemokine ligand 12/C-X-C chemokine receptor 4) coordinate epithelial–mesenchymal transition, stemness, chemotaxis, and vascular remodeling. Building on these insights, this review also argues for subtype-specific biomarkers and multimodal therapeutic strategies to overcome stromal-mediated resistance. Integrating stromal heterogeneity into precision-oncology workflows through standardized, lineage-resolved profiling and real-time biomarker guidance will be essential for diagnostic refinement and personalized treatment.

Introduction

Stromal cells, once viewed as passive structural components, are now recognized as active regulators of cancer progression within the tumor microenvironment (TME) [1]. Single-cell spatial multiomics have delineated 4 conserved cancer-associated fibroblast (CAF) subtypes with distinct niches and functions. Tumor-proximal S1-CAFs drive extracellular matrix (ECM) remodeling and immunosuppression through collagen type I alpha 1 chain (COL1A1), actin alpha 2 (ACTA2), and transforming growth factor-beta 1 (TGF-β1). S2-CAFs, enriched in stromal regions, secrete interleukin-6 (IL-6) to drive inflammation. Perivascular S3-CAFs mediate stromal–immune cross-talk via platelet-derived growth factor receptor (PDGFR) and matrix metalloproteinase 2 (MMP-2). S4-CAFs within tertiary lymphoid structures (TLSs) modulate adaptive immunity via human leukocyte antigen (HLA) class II molecules and chemokines such as C-X-C motif chemokine ligand 9 (CXCL9) and C-C motif chemokine ligand 21 (CCL21) [2].

Beyond CAFs, hepatic stellate cells (HSCs) in hepatocellular carcinoma (HCC) exhibit plasticity between tumor-promoting myofibroblastic (myHSC) and cytokine-secreting inhibitory (cyHSC) states [3]. Stromal–tumor cross-talk is exemplified by semaphorin 3C (SEMA3C) from HCC cells activating HSCs via neuropilin-1 (NRP1) and integrin β1 (ITGB1), inducing IL-6 release and cholesterol biosynthesis. Conversely, CAF-derived TGF-β1 up-regulates SEMA3C in cancer stem cells (CSCs), establishing a feed-forward protumorigenic circuit that contributes to therapy resistance, including sorafenib-resistant HCC [4].

Traditional bulk omics approaches obscure stromal heterogeneity and spatial context. In contrast, single-cell and spatial multiomics, such as graph-based integration of gene expression, spatial coordinates, and molecular interactions, enable precise alignment of transcriptomic, proteomic, and spatial layers to define stromal subtypes, map cell–cell communication, and resolve niche-specific behaviors [5]. These methods reveal spatially organized stromal-immune zones and context-dependent functions, critical for understanding tumor progression.

This review therefore catalogs stromal subtypes, elucidates their mechanisms, maps spatial niches, and translates these insights into clinical strategies. We further evaluate emerging stromal-targeted therapies, propose new avenues for intervention, and highlight prognostic stromal signatures as biomarkers for precision oncology.

Discovery of Stromal Cell Heterogeneity through Single-Cell Spatial Multiomics

Core technologies and principles

Spatial transcriptomics platforms such as 10x Genomics Visium and NanoString GeoMx Digital Spatial Profiler enable high-resolution gene-expression profiling in intact tissues, addressing the loss of spatial context inherent to single-cell RNA sequencing (scRNA-seq). Visium provides transcriptome-wide, barcoded capture suitable for unbiased discovery of stromal subtypes, e.g., IL-6-expressing S2-CAFs, and for mapping their distribution relative to tumor nests or TLSs [6]. In contrast, GeoMx performs immunohistochemistry-guided, region-of-interest profiling of ~50 to 1,800 genes/proteins, offering high sensitivity for validating low-abundance stromal markers (e.g., CXCL9 in S4-CAFs) within defined niches [2].

Single-cell proteomics platforms, including mass cytometry (CyTOF) and multiplexed ion beam imaging by time-of-flight (MIBI-TOF), complement spatial transcriptomics by quantifying protein expression and post-translational modifications [7]. CyTOF enables high-parameter phenotyping to resolve functionally distinct stromal subsets (e.g., profibrotic versus immunosuppressive HSCs), whereas MIBI-TOF affords subcellular spatial resolution to visualize protein colocalization and cell–cell interactions such as HLA-DR$^+$ S4-CAFs engaging T cells within lymphoid structures [8,9]. Computational integration using tools such as Seurat and stKeep aligns transcriptional, proteomic, and spatial coordinates to define stromal subtypes by gene programs, functional protein activity, and anatomical location, thereby enabling precise mapping of cell–cell communication and niche-specific behaviors [10].

Despite their transformative impact, single-cell and spatial multiomics technologies have important limitations that can bias stromal subtype inference and niche interpretation. For scRNA-seq, tissue dissociation itself can induce artifactual stress-response programs and alter cell-state-defining transcripts, potentially confounding cytokine-axis attribution or stromal activation signatures [11]. In solid tumors, dissociation conditions (e.g., collagenase) can trigger conserved stress responses, and cold-active protease protocols reduce these dissociation-associated transcriptional artifacts, underscoring the need for standardized processing when comparing stromal states across cohorts [12]. Droplet-based assays are additionally affected by ambient RNA contamination, which can create misleading marker detection in stromal and immune compartments unless explicitly modeled and removed [13]. For spatial transcriptomics, a major constraint of widely used spot-based platforms is multicell mixing within each spatial unit, which can blur tumor–stroma boundaries and inflate apparent stromal–immune coexpression; deconvolution methods such as RCTD and cell2location can partially recover cell-type composition but remain sensitive to reference quality and cross-platform effects [14]. More broadly, spatially resolved transcriptomics involves trade-offs between sensitivity, transcriptome coverage, and resolution, and field-facing discussions highlight these constraints as central to experimental design [15].

Applications of multiomics in stromal cell research

A long-standing challenge in stromal biology is the in vitro–in vivo disconnect. Stromal cells cultured in conventional 2-dimensional/3-dimensional (2D/3D) systems frequently lose native phenotypes and functional networks, thereby compromising their relevance to actual tumor biology [16]. Figure 1 contextualizes how multiomics addresses this issue: Fig. 1A details the workflow of integrating scRNA-seq from dissociated tumor cells and spatial transcriptomics from hematoxylin and eosin (H&E)-stained tissue sections to characterize stromal cells within the intact TME; Fig. 1B depicts CAF phenotyping into "good prognostic" (e.g., inflammatory cancer-associated fibroblast [iCAF] and interferon-response cancer-associated fibroblast [ifnCAF]) and "poor prognostic" (e.g., tumor-like cancer-associated fibroblast [tCAF] and matrix cancer-associated fibroblast [mCAF]) subtypes, alongside their roles in tumor–immune interactions (e.g., immune infiltration vs. exclusion). Leveraging single-cell spatial multiomics enables detailed TME characterization to guide the development of physiologically representative in vitro models [17].

Another well-documented issue is culture-induced convergence driven by nonphysiologic mechanics. Under standard tissue-culture conditions, patient-derived CAFs rapidly lose tumor-specific subset distinctions and converge toward a wound-healing/myofibroblastic state within a few passages [18]. This drift is exacerbated by the supraphysiologic stiffness of tissue-culture polystyrene, which pushes fibroblasts toward activation programs [19]. Conversely, microengineered niches (e.g., micropatterning and tunable-stiffness hydrogels) can re-establish in vivo-like CAF programs, yielding desmoplastic versus inflammatory phenotypes and improving drug-response fidelity [20]. Consistent with these findings, epithelial cues are required to sustain specific CAF states in pancreatic ductal adenocarcinoma (PDAC). Epithelial mitogen-activated protein kinase (MAPK)–TGF-β signaling and epidermal growth factor receptor (EGFR)/ERBB2 activation help maintain myofibroblastic CAF programs, underscoring why monoculture conditions lacking these signals promote dedifferentiation [21,22].

Multiomics also uncovers stromal-immune mechanisms that are absent in vitro. Immunosuppressive CAF functions are often lost under conventional culture conditions due to the lack of spatial context. MIBI-TOF revealed that in vivo, S1-CAFs deposit dense collagen (COL1+) and express programmed death-ligand 1 (PD-L1), forming both a physical and inhibitory barrier to T cells [23,24]. In vitro, these traits are diminished. Incorporating ECM scaffolds and vascular endothelial cells into 3D cocultures restores PD-L1 expression and immunosuppressive functionality, as confirmed via CyTOF analyses [25,26].

Multiomics has fundamentally revised our understanding of stromal plasticity. By integrating single-cell transcriptomics with tissue- and protein-level readouts, recent atlases resolve HSCs not as a uniformly myofibroblastic fate but as a conserved activation continuum that bifurcates into 2 in vivo-stable states: a matrix-producing, TGF-β/SMAD-driven myofibroblastic program (myHSC; αSMA/ACTA2$^+$ and COL1A1$^+$) and a cytokine-secreting, tumor-constraining program (cyHSC; e.g., IL-10$^+$ and TGFB1$^-$) [27]. This multiomics framework reframes experimental design and identifies therapeutic opportunities to rebalance HSC states or interrupt state-specifying axes, limiting matrix-driven tumor promotion while sparing protective cytokine functions [9].

Multiomics now predicts therapy response by resolving stromal subtypes and their niches. In HCC, enrichment of POSTN$^+$ CAFs identified by integrated single-cell/spatial analyses predicted diminished benefit from anti-programmed cell death protein 1 (PD-1)/PD-L1, nominating POSTN$^+$ stroma as a resistance biomarker and target [28]. In colorectal cancer, spatial transcriptomics of the tumor–stroma boundary showed CXCL14$^+$ CAF-rich, collagen-remodeling barriers in nonresponders, whereas LAMP3$^+$ dendritic cells and CXCL13$^+$ T-cell niches marked

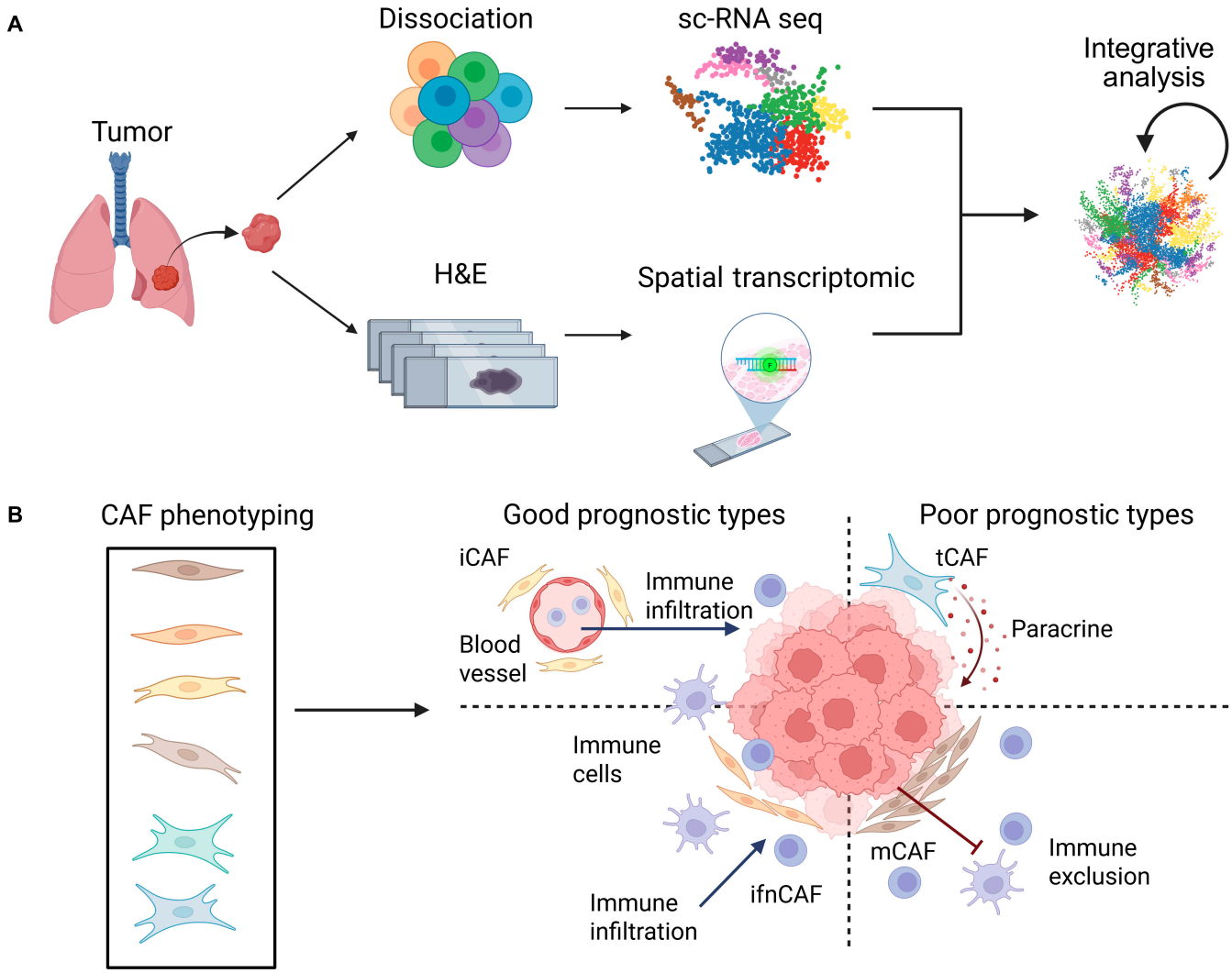


Fig. 1. Single-cell spatial multiomics workflow for decoding stromal cell heterogeneity in TME. (A) Integrative analysis of single-cell RNA sequencing (scRNA-seq) and spatial transcriptomics from tumor tissue. (B) Phenotyping of cancer-associated fibroblasts (CAFs) and their roles in tumor microenvironment immune regulation. ifnCAF, interferon-response CAF; tCAF, tumor-like CAF; iCAF, inflammatory CAFs; mCAF, matrix CAF.

responders, linking stromal states to checkpoint blockade efficacy [29]. Complementarily, a tumor–immune barrier signature in HCC derived from multiomic profiling predicted immunotherapy responses, underscoring that stromal architecture captured by multiomics is clinically actionable [30]. The major stromal lineages/subtypes in the TME are concluded in Table 1.

Heterogeneity and Functional Roles of Major Stromal Cell Populations in TME

Cancer-associated fibroblasts

CAFs are abundant and highly plastic stromal cells that remodel ECM, modulate inflammatory cues, and influence antitumor immunity across solid tumors. Single-cell and spatial multiomics analyses have converged on 4 conserved CAF archetypes with distinct transcriptional programs and spatial niches, as illustrated by the diverse CAF subsets (e.g., myCAFs, iCAFs, apCAFs, tCAFs, ifnCAFs, pCAFs, and rCAFs) and their signature markers in Fig. 2A. Myofibroblastic CAFs (myCAFs) express ACTA2 and TAGLN, concentrate at tumor–stromal interfaces, and specialize in matrix deposition and contractility, while iCAFs secrete cytokines such as IL-6 and chemokines like CXCL12 and can interconvert with myCAFs through opposing IL-1–Janus kinase/signal transducer and activator of transcription (JAK/STAT) and TGF-β–SMAD signaling [31]. Antigen-presenting CAFs (apCAFs) upregulate MHC-II and CD74 yet lack classical costimulation, enabling cognate interactions with $CD4^+$ T cells that tend to be tolerogenic, and lineage tracing indicates that mesothelial cells can give rise to apCAFs during pancreatic tumor progression [32]. Vascular-associated CAFs (vCAFs) are defined by markers including MCAM, NOTCH3, and COL18A1; reside near microvessels; and exemplify perivascular cross-talk through NOTCH3-programmed stromal activation that enhances collagen production and invasion in lung adenocarcinoma [33]. Large pan-cancer spatial atlases integrating transcriptomic and proteomic platforms validate these 4 CAF states as conserved and spatially organized neighborhoods, linking subtype composition to immune contexture and clinical outcomes. Collectively, this framework supports subtype-aware therapeutic strategies that target TGF-β/ECM programs or disrupt pathogenic NOTCH signaling in selected contexts [34].

Table 1. Major stromal lineages/subtypes in the TME: markers, spatial niches, functions, exemplar contexts, and key evidence. ↑ denotes "expression up-regulation" (gene/protein levels significantly higher than those in other TME stromal cells or normal counterparts), while ↓ denotes "expression down-regulation" (gene/protein levels significantly lower than those in other TME stromal cells or normal counterparts).

Cell subtype	Representative markers	Typical spatial niche	Core functions/ phenotypes	Tumor cite	Key references
myCAF (myofibroblastic)	ACTA2/α-SMA, TAGLN, COL1A1	Tumor borders, invasive fronts	ECM synthesis/ contractility; matrix stiffening	PDAC (pancreas)	[31]
iCAF (inflammatory)	IL-6↑, CXCL12↑, PDGFRA	Interstitial stroma away from nests	JAK/STAT3 inflammatory circuits; cytokine/ chemokine exchange with tumor cells	PDAC (pancreas)	[31]
apCAF (antigen-presenting)	MHC-II, CD74 (low costimulation)	Near tumor nests/ TLS rims	Cognate but tolerogenic $CD4^+$ T-cell interactions; mesothelial contribution	PDAC	[32]
vCAF (vascular-associated)	NOTCH3, NR2F2, EPAS1, COL18A1	Perivascular sleeves	NOTCH3-programmed stromal activation; collagen deposition; invasion	Lung adenocarcinoma	[33]
FAP^+ CAFs (functional bucket)	FAP, CXCL12	Stromal rims and fibrotic zones	Immune exclusion; targetable for imaging/therapy	PDAC; GI; breast	[158]
ifnCAF (interferon-response CAF)	IDO, CXCL9, CXCL10, CXCL11, IL-32	Tumor–stroma interface; closest to tumor cells in IMC	IFN-response program; associated with inflamed TME and favorable prognosis	Breast; NSCLC	[17,33]
tCAF (tumor-like CAF)	PDPN, MME (CD10), ENO1, NDRG1, CA9 (including stress/ hypoxia-like states)	Tumor–stroma interface; frequent tumor contact	Tumor growth/ angiogenesis-like program; associated with poor prognosis	Breast; NSCLC	[17,33]
mCAF (matrix CAFs)	MMP-11, CDH11, POSTN, collagen genes	Throughout stroma	ECM/stromal maintenance; linked to immune-poor stroma and worse survival	Breast; NSCLC	[17,33]
$POSTN^+$ CAF neighborhoods (HCC barrier-associated)	POSTN (often α-SMA^+); IL-6 ligand activity; ECM/TGF-β programs	Spatial tumor immune barrier regions	T-cell exclusion; IL-6–STAT3 coupling to $SPP1^+$ macrophages; reduced ICI benefit	HCC	[28]
$CXCL14^+$ CAF-rich collagen-remodeling barrier (CRC boundary)	CXCL14 (often $COL1A1^+CXCL14^+$); boundary ECM program (including MMP-11 induction via IHH–PTCH1)	Tumor–stroma boundary ($\approx 0 \pm 150$ μm)	Structural barrier in nonresponders; contrasts with immune-activating boundary ($LAMP3^+$ DC/CXCL13 signaling)	CRC	[29]
S1-CAF (matrix/ immune-suppressive rim)	COL1A1, PD-L1, TGFB1	Tumor–stroma interface; dense collagen rims	Physical + immunologic barrier; EMT priming	Multiple solids	[2]

(Continued)

Table 1. (Continued)

Cell subtype	Representative markers	Typical spatial niche	Core functions/ phenotypes	Tumor cite	Key references
S2-CAF (inflammatory neighborhood)	IL6↑	Stromal zones away from nests	STAT3-driven inflammatory loops	Pan-cancer	[2]
S3-CAF (perivascular)	PDGFR, MMP-2	Vessel-adjacent	Stromal–immune cross-talk; perivascular remodeling	Pan-cancer	[2]
S4-CAF (TLS-related)	HLA-II, CXCL9, CCL21	Tertiary lymphoid structures	Adaptive-immunity modulation	Pan-cancer	[2]
TAECs (proliferative/ angiogenic)	VEGFR2/KDR, ANGPT2	Hypoxic/angiogenic fronts	Sprouting angiogenesis	Multiple solids	[39]
TAECs (quiescent/ steady)	CD36, ESAM; FA-transport/ junctional genes	Stable capillaries	Barrier and nutrient transport homeostasis	Multiple solids	[39]
TAECs (abnormal/ leaky)	↓VE-cadherin (CDH5), ↓CLDN5	Peri-necrotic/ EMT-active zones	Barrier failure; chaotic flow; intravasation	Multiple solids	[42]
Pericytes (contractile)	ACTA2, MYH11, TAGLN	Enwrapping microvessels	Flow regulation; vessel stability	Pan-cancer	[44]
Pericytes (noncontractile/ proangiogenic)	↓ACTA2/MYH11; ↑ECM/GF (e.g., ANGPT axes)	Angiogenic fronts	Sprouting support at cost of stability	Pan-cancer	[45]
Myofibroblastic hepatic stellate cells (myHSCs)	ACTA2, COL1A1	HCC stroma	ECM production; tumor-promoting	HCC	[27]
Cytokine-expressing hepatic stellate cells (cyHSCs)	IL-10^{+}/ TGFB1^{-} (context-dependent)	HCC stroma	Cytokine-secreting, tumor-constraining program	HCC	[27]

TME, tumor microenvironment; CAF, cancer-associated fibroblast(s); myCAF, myofibroblastic cancer-associated fibroblast(s); iCAF, inflammatory cancer-associated fibroblast(s); apCAF, antigen-presenting cancer-associated fibroblast(s); vCAF, vascular-associated cancer-associated fibroblast(s); FAP, fibroblast activation protein; GI, gastrointestinal; ifnCAF, interferon-response cancer-associated fibroblast(s); IFN, interferon; IDO1 (IDO), indoleamine 2,3-dioxygenase 1; CXCL9, C-X-C motif chemokine ligand 9; CXCL10, C-X-C motif chemokine ligand 10; CXCL11, C-X-C motif chemokine ligand 11; IL-32, interleukin-32; IMC, imaging mass cytometry; NSCLC, non-small cell lung cancer; tCAF, tumor-like cancer-associated fibroblast(s); mCAF, matrix cancer-associated fibroblast(s); POSTN, periostin; HCC, hepatocellular carcinoma; ICI, immune checkpoint inhibitor(s); CRC, colorectal cancer; PDAC, pancreatic ductal adenocarcinoma; TNBC, triple-negative breast cancer; ACTA2, actin alpha 2 (smooth muscle); α-SMA, alpha-smooth muscle actin; TAGLN, transgelin; COL1A1, collagen type I alpha 1 chain; ECM, extracellular matrix; IL-6, interleukin-6; CXCL12, C-X-C motif chemokine ligand 12 (stromal cell-derived factor 1, SDF-1); SDF-1, stromal cell-derived factor 1; CXCR4, C-X-C chemokine receptor type 4; PDGFRA, platelet-derived growth factor receptor alpha; JAK, Janus kinase; STAT3, signal transducer and activator of transcription 3; MHC-II, major histocompatibility complex class II; CD74, cluster of differentiation 74 (invariant chain); TLS, tertiary lymphoid structure; CD4, cluster of differentiation 4; NOTCH3, neurogenic locus notch homolog 3; NR2F2, nuclear receptor subfamily 2 group F member 2 (COUP-TFII); EPAS1, endothelial PAS domain protein 1; HIF-2α, hypoxia-inducible factor 2 alpha; COL18A1, collagen type XVIII alpha 1 chain; PDPN, podoplanin; MME (CD10), membrane metallo-endopeptidase (cluster of differentiation 10); ENO1, enolase 1; NDRG1, N-myc downstream regulated gene 1; CA9, carbonic anhydrase 9; MMP-11, matrix metalloproteinase 11; CDH11, cadherin 11; TGF-β, transforming growth factor-beta; TGFB1, transforming growth factor-beta 1; SPP1, secreted phosphoprotein 1 (osteopontin); FOXP3, forkhead box P3; Treg, regulatory T cell(s); CXCL14, C-X-C motif chemokine ligand 14; IHH, Indian hedgehog; PTCH1, patched 1; LAMP3, lysosomal-associated membrane protein 3; DC, dendritic cell(s); CXCL13, C-X-C motif chemokine ligand 13; PD-L1, programmed death-ligand 1; EMT, epithelial–mesenchymal transition; S1-CAF, state-1 cancer-associated fibroblast (matrix/immune-suppressive rim); S2-CAF, state-2 cancer-associated fibroblast (inflammatory neighborhood); S3-CAF, state-3 cancer-associated fibroblast (perivascular); S4-CAF, state-4 cancer-associated fibroblast (tertiary lymphoid structure-related); PDGFR, platelet-derived growth factor receptor; MMP-2, matrix metalloproteinase 2; HLA-II, major histocompatibility complex class II (human leukocyte antigen class II); CCL21, C-C motif chemokine ligand 21; TAECs, tumor-associated endothelial cells; TAEC, tumor-associated endothelial cell; TEC, tumor endothelial cell; VEGFR2, vascular endothelial growth factor receptor 2; KDR, kinase insert domain receptor (VEGFR2); ANGPT2, angiopoietin 2; CD36, cluster of differentiation 36 (fatty-acid translocase); ESAM, endothelial cell-selective adhesion molecule; FA, fatty acid; VE-cadherin, vascular endothelial cadherin; CDH5, cadherin 5; CLDN5, claudin 5; MYH11, myosin heavy chain 11; ANGPT, angiopoietin; GF, growth factor; myHSCs, myofibroblastic hepatic stellate cells; cyHSCs, cytokine-expressing hepatic stellate cells; IL-10, interleukin-10

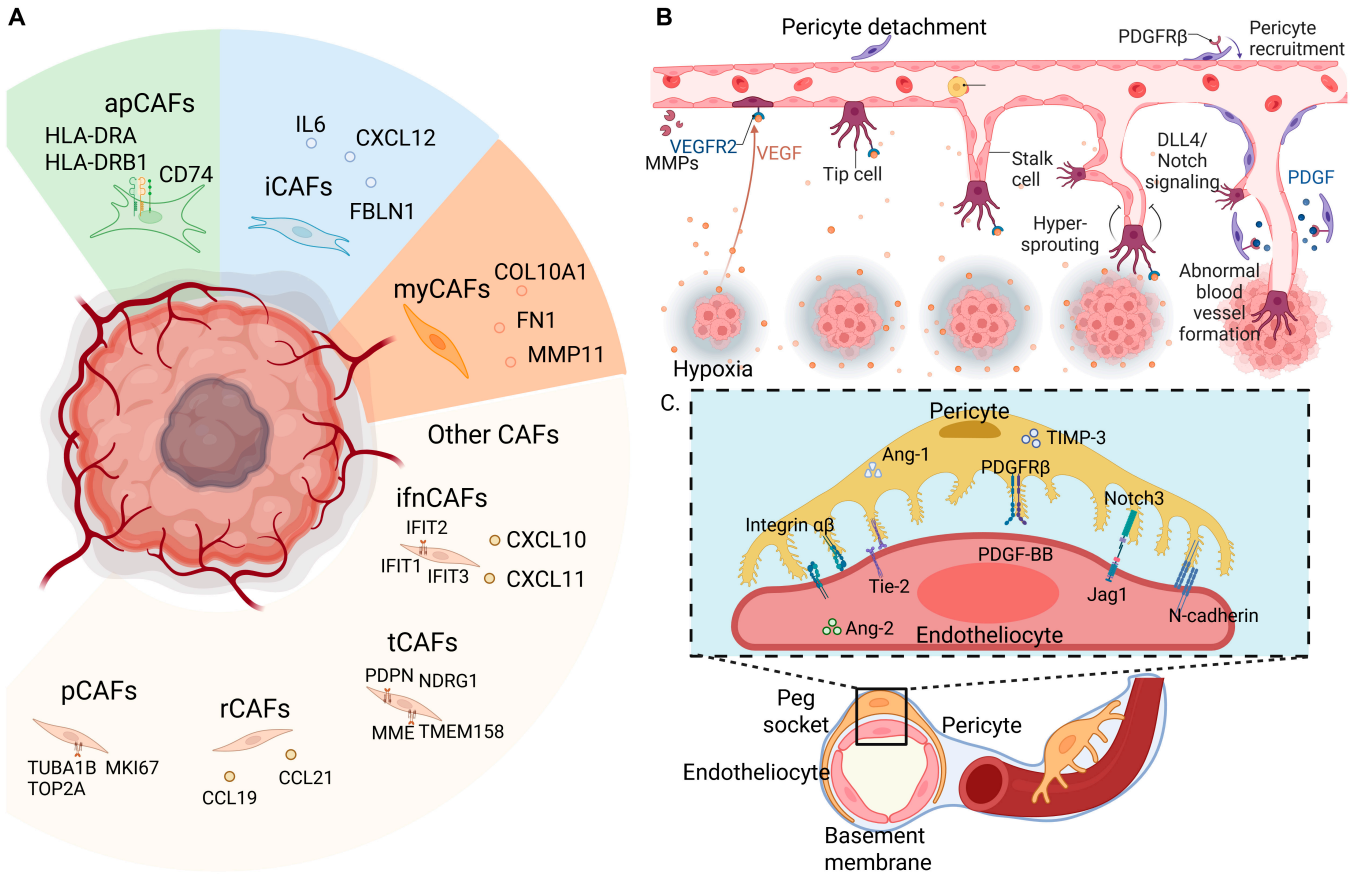


Fig. 2. Stromal heterogeneity and spatial niches across the TME. (A) Heterogeneous cancer-associated fibroblast (CAF) subsets with distinct marker genes. (B) Pathological vascular formation involving pericyte detachment.(C) Physiological pericyte–endotheliocyte cross-talk in vascular homeostasis.

Vascular endothelial cells

Tumor-associated endothelial cells (TAECs) within the TME display marked functional and molecular heterogeneity beyond their conventional role in the blood circulation, as shown in Fig. 2B [35]. Single-cell transcriptomics has identified several distinct TAEC subpopulations: proliferative TAECs, which express VEGFR2 and angiopoietin-2 and localize to angiogenic regions such as the invasive front and hypoxic niches [36]. A quiescent state is enriched in vessels with stable junctions and higher expression of fatty-acid transport and junctional programs, exemplified by CD36 in capillary endothelium and tight-junction molecules such as ESAM in homeostatic vessels [37]. An abnormal state shows reduced VE-cadherin and claudin-5 with barrier failure, driving leakiness that facilitates intravasation, extravasation, and disordered flow [38]. TAECs also perform diverse functions including the formation of the blood–tumor barrier, which exhibits altered permeability affecting drug delivery and immune infiltration [39]. They also rewire nutrient trafficking to buffer metabolic stress and support tumor bioenergetics [40]. In metastatic seeding, endothelial E-selectin promotes arrest and adhesion of circulating tumor cells, and angiocrine signals from endothelium foster colonization competence [41]. Spatially, TAEC composition tracks progression, with proliferative TAECs increased in advanced or hypoxic regions of solid tumors [36]. Abnormal TAECs frequently align with perinecrotic zones or epithelial–mesenchymal transition (EMT)-active territories in which leakiness and angiogenic remodeling colocalize [42]. This evolving heterogeneity highlights stage-aware vascular strategies that pair normalization or anti-angiogenic agents with immunotherapy or metabolism-targeted approaches.

Pericytes

Recent multiomics technologies have uncovered significant heterogeneity in pericytes within the TME [43]. Two main subtypes have been identified, as contractile pericytes, which express high levels of α-SMA/ACTA2 and SM-MHC/MYH11, enwrap microvessels, and regulate blood flow through contraction [44], and noncontractile pericytes, which exhibit reduced contractility but produce ECM components and growth factors and often localize to angiogenic fronts to support neovessel formation [45]. Signaling pathways such as TGF-β, Notch, and Wnt regulate transitions toward a less-contractile, proangiogenic phenotype that promotes vessel growth at the expense of vascular stability [46].

Pericytes maintain intimate cross-talk with endothelial cells via key molecular pathways, as detailed in the molecular interactions between pericytes and endothelial cells in Fig. 2C. The PDGF-BB/PDGFR-β axis mediates pericyte recruitment and vessel coverage, while pericyte-derived angiopoietin-1 activates endothelial Tie2 receptors to enhance junctional integrity [47]. Through gap junctions and paracrine signals including TGF-β and vascular endothelial growth factor (VEGF), pericytes further modulate vascular permeability and stability, and dysregulation of these interactions in tumors contributes to abnormal vessel function and leakage [48].

Beyond structural roles, pericytes actively facilitate metastasis. Detachment from vessels, driven by protease activity,

signaling imbalances, or mechanical stress, creates gaps that promote tumor cell intravasation and extravasation [49]. Detached pericytes can transition into CAFs and secrete proinvasive mediators such as TGF-β and CCL2 that foster EMT and invasion [50]. Moreover, pericytes contribute to premetastatic niche formation via matrix remodeling and cytokine secretion [51]. Low pericyte coverage correlates with poor prognosis and heightened metastatic risk in several settings, underscoring their role as active mediators of cancer dissemination rather than mere structural supporters [52].

Tumor-type-specific stromal ecosystems

While pan-cancer single-cell/spatial atlases support a conserved stromal backbone, the relative abundance, spatial deployment, and immune coupling of stromal programs vary markedly by tumor type, creating tissue-specific stromal ecosystems with distinct therapeutic implications. In PDAC, desmoplasia is dominated by spatially segregated fibroblast programs, including tumor-interface myCAFs and more interstitial iCAFs, which can interconvert under opposing IL-1–JAK/STAT versus TGF-β–SMAD cues. PDAC also features apCAFs enriched near tumor/TLS-like rims, supporting tolerogenic $CD4^+$ T-cell interactions [31,32]. In HCC, stromal architecture is strongly shaped by HSC state continua, including matrix-producing myofibroblastic HSC (myHSC) programs versus cytokine-expressing, potentially tumor-constraining states, emphasizing that CAF-like activation in liver cancers has a lineage-specific backbone [27]. Multiomics further links HCC stroma to immunotherapy outcomes: enrichment of $POSTN^+$ CAF neighborhoods and tumor immune barrier features correlates with reduced benefit from anti-PD-1/PD-L1, nominating specific stromal states as predictive resistance biomarkers and targets [28,30]. In breast cancer, spatial profiling reveals pronounced plasticity of immunosuppressive fibroblast neighborhoods and their alignment with immune exclusion patterns, reinforcing that fibroblast-mediated suppression can be organized into discrete spatial programs rather than diffuse activation [53]. Finally, in CRC, spatially organized tumor–stroma boundaries can stratify immunotherapy response, where $CXCL14^+$ CAF-rich collagen-remodeling barriers are enriched in nonresponders, whereas responder regions show immune-activating niches (e.g., $LAMP3^+$ DC and $CXCL13^+$ T-cell neighborhoods), directly connecting boundary stromal states to clinical efficacy [29].

These tumor-type differences imply that stromal interventions should be tumor-specific and niche-aware rather than uniformly CAF-targeted. In PDAC, barrier-like myCAF-rich rims and cytokine/chemokine circuits from iCAFs/apCAFs plausibly contribute to immune exclusion and poor drug penetration, suggesting that combination strategies may need to match the dominant local program (ECM/TGF-β-skewed versus inflammatory IL-6/CXCL12-skewed) identified by single-cell/spatial readouts [31,32]. In HCC, multiomics-defined barrier states (e.g., $POSTN^+$ CAF enrichment and immune-barrier signatures) provide a rationale for patient stratification and for pairing checkpoint blockade with stromal reprogramming aimed at dismantling barrier-like niches [28,30]. In breast cancer/TNBC, treatment-induced remodeling of stromal–immune circuits can follow distinct response trajectories under immunotherapy-based regimens, emphasizing that stromal states are dynamic and may require on-treatment monitoring rather than one-time pretreatment labeling [54]. In CRC, the spatial logic of the tumor–stroma boundary offers a practical framework to interpret why otherwise similar tumor-intrinsic features yield different immunotherapy outcomes, and motivates boundary-targeted stromal normalization to unlock immune infiltration [29]. Collectively, these findings justify adding a tumor-type-resolved stromal ecosystem layer on top of conserved subtype taxonomies, and we summarize the corresponding stromal–immune cross-talk in a single-cell-resolved schematic (Fig. 3).

Mechanisms of Stromal Cell-Derived Cytokines in Regulating Tumor Metastasis

Key cytokine signaling axes mediating CAF-tumor cell cross-talk

Cytokine-mediated communication between CAFs and tumor cells is a fundamental driver of metastatic progression, orchestrating processes from local invasion to distant colonization [50]. The TGF-β pathway serves as a central regulator in this stromal–tumor cross-talk, integrating canonical SMAD signaling with noncanonical cascades [55]. CAF-derived TGF-β activates SMAD-dependent and MAPK/phosphoinositide 3-kinase (PI3K)–protein kinase B (AKT) signaling in tumor cells, inducing EMT through E-cadherin loss and up-regulation of N-cadherin, vimentin, and EMT-TFs such as Snail and Twist [56]. Concurrently, TGF-β programs CAFs to enhance matrix remodeling by up-regulating MMP-2 and MMP-9 that facilitate ECM degradation and promotes collagen cross-linking via lysyl-oxidase family enzymes, yielding a stiffened matrix that supports invasion through mechanosensing [57].

IL-6 signaling in the CAF–tumor axis centers on the IL-6R/gp130 complex, which robustly activates JAK/signal transducer and activator of transcription 3 (STAT3) and also engages the PI3K/AKT pathway. AKT, in turn, functionally inhibits GSK3β, converging on prostemness and prosurvival programs [58,59]. In cancer cells, CAF-derived IL-6 phosphorylates STAT3 and up-regulates stemness drivers (NANOG, OCT4, and SOX2), a phenotype linked to therapy resistance [60,61]. STAT3 also promotes apoptosis evasion by transcriptionally inducing anti-apoptotic effectors such as BCL-2 and MCL-1 [62,63]. Moreover, STAT3 cooperates with NF-κB and HIF-1α to create a self-reinforcing inflammatory–hypoxic loop that sustains metastatic signaling [64,65].

At the vascular interface, IL-6 trans-signaling (via sIL-6R) activates STAT3/AKT/ERK in endothelial cells and up-regulates adhesion/coagulation cues linking local tumor cytokine flux to vascular effects [66,67]. Systemically, classic IL-6 signaling in hepatocytes is a principal driver of the acute-phase response (e.g., C-reactive protein and fibrinogen), thereby connecting paracrine tumor IL-6 to hepatic and circulatory consequences; notably, sgp130-Fc selectively blocks IL-6 trans-signaling [68].

Metastatic dissemination is reinforced by a layered network of cytokine and growth-factor signals that operate in parallel and with substantial redundancy. The CXCL12–CXCR4 axis directs tumor-cell homing to permissive niches such as bone marrow [69,70], and hepatocyte growth factor (HGF)–MET signaling promotes collective migration and survival via the adaptor GAB1, activating downstream PI3K–AKT/MAPK pathways [71]. Functionally, these partially overlapping circuits safeguard metastatic competence even under therapeutic pressure by preserving motility, survival, and niche adaptation.

Within desmoplastic PDAC, CAF-derived leukemia inhibitory factor–leukemia inhibitory factor receptor signaling augments chemoresistance and may be leveraged alongside cytotoxic

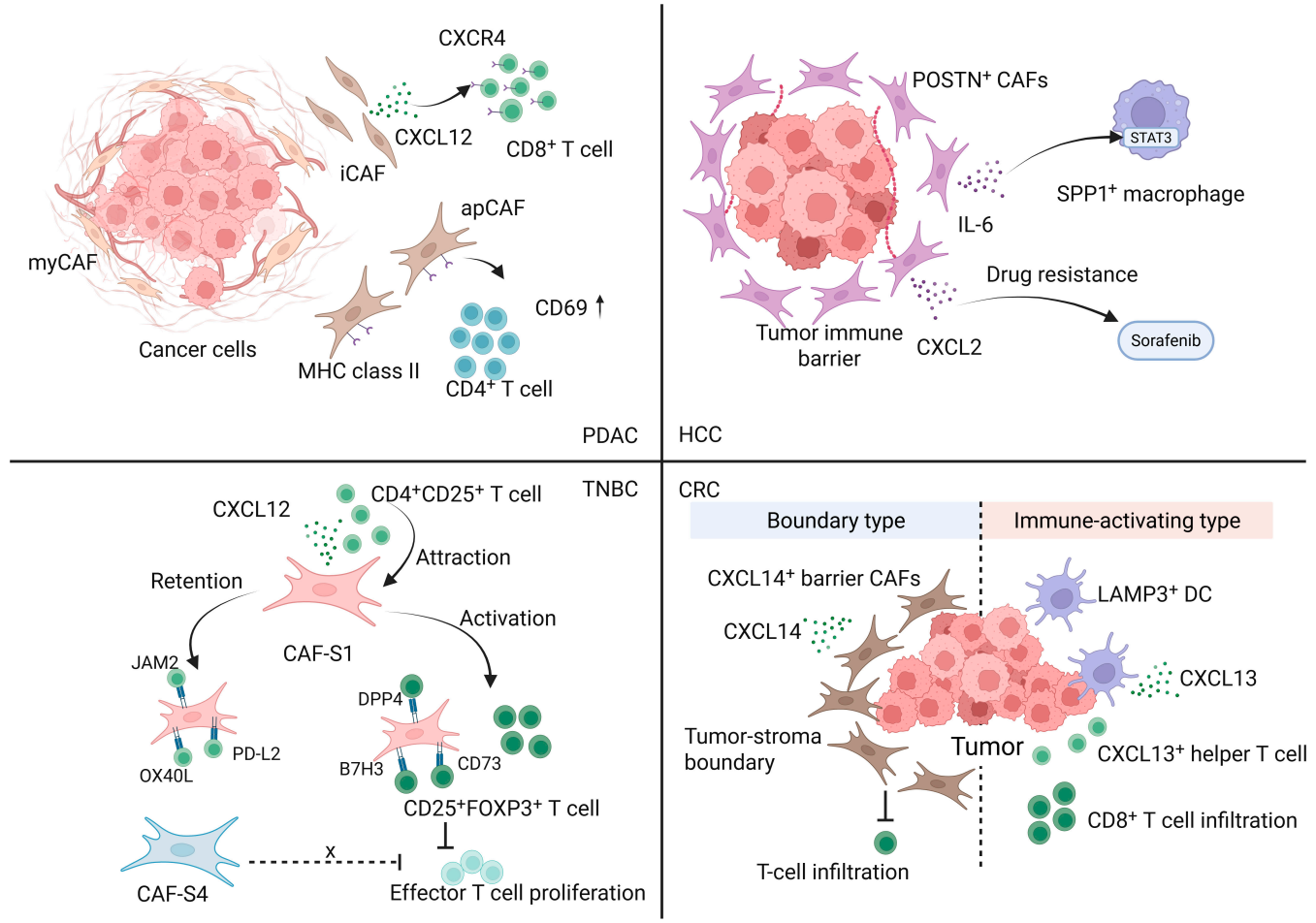


Fig. 3. Tumor-type-specific stromal–immune circuits shaping immune exclusion and therapeutic response. Schematic overview of representative stromal niches across tumor types. PDAC: myCAF/iCAF programs contribute to barrier formation; iCAFs signal via CXCL12–CXCR4 to promote T-cell exclusion; apCAFs express MHC-II and engage $CD4^+$ T cells. HCC: $POSTN^+$ CAFs form a spatial immune barrier and activate an IL-6–STAT3 axis in $SPP1^+$ macrophages, linking myeloid immunosuppression to therapy resistance. TNBC: CAF-S1 attracts/retains $CD4^+CD25^+$ T cells via CXCL12 and promotes $FOXP3^+$ Treg-skewing through additional ligand–receptor interactions. CRC: tumor–stroma boundary states stratify ICI outcomes, with $CXCL14^+$ barrier CAFs limiting infiltration versus an immune-activating boundary enriched for $LAMP3^+$ DC/CXCL13 signaling that supports T-cell entry. PDAC, pancreatic ductal adenocarcinoma; HCC, hepatocellular carcinoma; TNBC, triple-negative breast cancer; CRC, colorectal cancer; CAF, cancer-associated fibroblast(s); myCAF, myofibroblastic cancer-associated fibroblast(s); iCAF, inflammatory cancer-associated fibroblast(s); apCAF, antigen-presenting cancer-associated fibroblast(s); CXCL12, C-X-C motif chemokine ligand 12 (stromal cell-derived factor 1, SDF-1); CXCR4, C-X-C chemokine receptor type 4; MHC-II, major histocompatibility complex class II; $CD4^+$ T cell, cluster of differentiation 4-positive T cell; $CD25^+$ T cell, cluster of differentiation 25-positive T cell (interleukin-2 receptor alpha-positive T cell); POSTN, periostin; IL-6, interleukin-6; STAT3, signal transducer and activator of transcription 3; SPP1, secreted phosphoprotein 1 (osteopontin); FOXP3, forkhead box P3; Treg, regulatory T cell(s); ICI, immune checkpoint inhibitor(s); CXCL14, C-X-C motif chemokine ligand 14; LAMP3, lysosomal-associated membrane protein 3; DC, dendritic cell(s); CXCL13, C-X-C motif chemokine ligand 13.

backbones [72]. In the same stressed stromal ecosystems, IL-11 acting through IL-11Rα/gp130–STAT3 further reinforces anti-apoptotic programs and EMT [73]. Inflammatory chemokine circuits add yet another layer: CXCL8/interleukin-8 (IL-8) engagement of CXCR1/2 maintains invasive, stem-like states and is the focus of active clinical efforts [74], while CCL5–CCR5 signaling promotes migration, invasion, and prometastatic conditioning across tumor types [75].

In parallel, receptor tyrosine kinase (RTK) programs provide fail-safe redundancy. GAS6–AXL supports EMT, invasion, and survival within hypoxic, invasive niches. Consistent with this theme, HGF–MET drives collective migration and pro-survival signaling via a GAB1-scaffolded PI3K–AKT/MAPK cascade. Conceptually, RTK coactivation broadens signaling bandwidth and guards against single-node therapeutic blockade [76].

Guidance cues further diversify the prometastatic signaling repertoire. In HCC, SEMA3C signaling through NRP1/ITGB1 establishes a bidirectional tumor–stellate/CAF loop that amplifies NF-κB/IL-6 programs and fosters therapy resistance [4]. SEMA4D–PLXNB1 can engage PI3K–AKT and cross-talk with c-MET in aggressive contexts [77], whereas SLIT2–ROBO1 shows tissue-specific duality, promoting PDAC liver outgrowth but restraining tumor programs in other settings [78]. These guidance pathways integrate positional information with stromal feedback, effectively tuning metastatic behavior to organ context.

At the tumor–stroma interface, CAF-derived morphogens orchestrate vascular, immune, and invasive phenotypes. WNT2 and WNT5A signaling through FZD and ROR receptors influences angiogenesis, immune evasion, and invasion [79]. Contact-dependent JAG1–NOTCH signaling at tumor–stroma interfaces

entrenches EMT, stemness, and context-dependent therapeutic resistance [80]. Additional growth-factor streams, including PDGF and FGF2 acting through FGFRs, drive proliferation, migration, and stromal remodeling in perivascular and fibrotic zones [81,82]. Extracellular-matrix-encoded signals such as osteopontin (OPN/SPP1) via CD44/integrins and periostin (POSTN) via αv-integrins promote stemness and metastatic competence within dense desmoplasia [83].

Epigenetic regulation is increasingly recognized as a key layer that couples microenvironmental cues to durable yet reversible stromal cell states, thereby enabling CAF plasticity and subtype switching. In PDAC, tumor cells can actively reprogram fibroblasts through induced DNA methylation programs, exemplified by methylation-dependent suppression of negative regulators (e.g., SOCS1) and downstream activation of protumor signaling such as STAT3, ultimately promoting tumor growth [84]. Complementarily, metabolic cues can directly reshape the CAF epigenome: tumor-derived lactate flux activates TET-dependent demethylation, leading to widespread loss of cytosine methylation and transcriptional rewiring during CAF formation [85]. Beyond DNA methylation, histone modifications provide an epigenetic memory that stabilizes tumor-promoting programs. In breast stroma, cancer cell exposure reduces EZH2 occupancy and H3K27 trimethylation at specific promoters (e.g., ADAMTS1), producing a heritable invasive CAF-like phenotype [86]. Consistently, loss of H3K27me3 in CAFs is enriched at genes encoding stem-cell niche and stromal–epithelial interaction factors and functionally associates with enhanced tumor-promoting capacity [87]. Importantly, chromatin readers/writers/erasers can be therapeutically leveraged to reprogram stroma: BET bromodomain inhibition (JQ1) disrupts TGF-β-dependent transcriptional machinery in CAFs and suppresses CAF activation programs in vivo, whereas histone deacetylase inhibition can paradoxically create a permissive chromatin landscape that unleashes AP-1-driven inflammatory (SASP-like) cytokine programs in CAFs, highlighting the need for rational combinations [88]. Finally, single-cell chromatin accessibility analyses provide direct evidence for state transitions (e.g., pre-CAF to CAF) and enhancer–gene links that underlie stromal lineage plasticity during malignant progression [89].

Finally, matrix remodeling consolidates the premetastatic state at the biophysical level. Lysyl oxidases (LOX/LOXL) stiffen and hypoperfuse the stroma while priming distant niches; pharmacologic pan-LOX inhibition (PXS-5505) can normalize mechanics and improve drug delivery in PDAC models [90,91]. This convergence of cytokine, RTK, guidance, morphogen, and matrix programs argue for rational, multiaxis therapeutic strategies that disrupt both biochemical signaling and biomechanical conditioning, with the aim of eroding metastatic readiness despite ongoing treatment pressure. The detailed information is shown in Table 2.

Spatial specificity of cytokine action

Stromal-derived cytokines' spatial distribution (via localized production, ECM sequestration, and concentration gradients) shapes the TME and metastatic progression [92]. Transforming growth factor-beta (TGF-β) concentrates at peritumoral rims and invasive fronts, where spatial profiling shows heightened TGF-β signaling and EMT programs relative to tumor cores, consistent with a peripherally polarized niche [93]. This polarization reflects stromal overproduction together with activation of latent TGF-β by proteases such as MMP-2 and MMP-9 and by αv-integrins that are enriched in invasion zones [94]. Latent TGF-β is tethered to ECM via LTBPs, creating a readily activatable reservoir that sustains gradients; interfering with matrix release of TGF-β confirms this reservoir function in situ [94]. Resultant TGF-β gradients drive EMT at the tumor–stroma interface and recruit or activate fibroblasts, amplifying a self-reinforcing TGF-β loop [95].

Interleukin-6 (IL-6) acts both locally and systemically [96]. Within primary tumors, it forms autocrine and paracrine loops between CAFs and tumor cells, sustaining STAT3 activation and stemness [61]. Systemically, IL-6 induces hepatic acute-phase proteins, such as serum amyloid A that prime premetastatic niches, and promotes prometastatic endothelial activation including adhesion-molecule up-regulation that facilitates tumor-cell arrest and transmigration [97]. IL-6 also intersects with bone remodeling by stimulating osteoclastogenic pathways through RANKL-dependent cues in the marrow ecosystem, thereby fostering skeletal colonization [98].

CXCL12 creates gradients guiding tumor cell migration. CAFs direct primary tumor cells toward blood vessels (aiding intravasation), while $CXCR4^{+}$ tumor cells home to CXCL12-producing organs (bone marrow: perivascular stromal cells/osteoblasts; lymph nodes: fibroblastic reticular cells), explaining organotropic metastasis [99]. Figure 4 visually encapsulates the molecular cascades underlying these events:

These spatial dynamics have therapeutic implications [100]. Localized TGF-β blockade using tumor-targeted nanovesicles or ECM-aware delivery can intensify effects at invasive fronts while mitigating systemic toxicity [101]. IL-6 inhibition generally requires systemic administration but must be balanced against infection risk and potential interference with antitumor immunity [102]. Targeting the CXCL12/CXCR4 axis benefits from temporal and spatial control because this pathway is indispensable for hematopoietic trafficking and broad chemokine homeostasis [103].

Multiomics evidence for cytokine-driven metastasis

Multiomics technologies have profoundly advanced our understanding of cytokine-driven metastasis, revealing specialized CAF subtypes that orchestrate prometastatic niches. Large pan-cancer spatial atlases now define conserved CAF programs whose abundance and neighborhoods correlate with immune state, therapy response, and survival [2]. Transcriptomic, proteomic, and spatial analyses consistently identify metastasis-promoting CAF signatures associated with poor clinical outcomes and therapeutic resistance. In melanoma and squamous cell carcinoma, spatial single-cell profiling resolves myofibroblastic, matrix, and immunomodulatory CAF states that expand with malignancy [104]. For pancreas, single-cell studies show functional CAF heterogeneity with myofibroblastic subsets that accelerate metastasis, while IL-1–IL1RAP signaling in CAFs drives chemokine output and neutrophil recruitment, directly tying inflammatory CAF circuits to dissemination [22]. Inflammatory axes extend to SAA family genes induced by IL-1 in CAFs, further linking stromal cytokines to neutrophil trafficking, and vascular-mimicry programs involve VE-cadherin (CD144)–β-catenin/TCF signaling that facilitates tumor channel formation and metastatic spread [105].

Functionally, these CAFs promote metastasis through extracellular-matrix remodeling and stemness induction (for example, via hyaluronan-rich niches that engage CD44), and by activating

Table 2. "Stroma → tumor" cytokine and guidance axes

Axis (class)	Stromal sources → Tumor targets (receptors)	Canonical downstream	Core biological effects	Spatial/ systemic features	Therapeutic notes	Key references
TGF-β (morphogen)	CAFs → tumor and CAFs (TβRI/II)	SMAD2/3/4; PI3K/AKT; MAPK	EMT, invasion, fibroblast activation; MMPs; collagen cross-talk	Steep gradients at stromal rims; latent ECM-tethered pools	Localized/ ECM-aware delivery; combo with IO/chemo	[55]
IL-6 (cytokine)	CAFs ↔ tumor (IL-6R/gp130)	JAK/STAT3; PI3K/AKT; GSK3β	Stemness, survival, acute-phase cues; EC activation	Tumor paracrine and systemic hepatic/ vascular effects	IL-6/IL-6R blockade; rational IO/chemo combinations	[58,59]
CXCL12/SDF-1 → CXCR4 (chemokine)	FAP^+ CAFs and stroma → $CXCR4^+$ tumor/ immune cells	PI3K/AKT; MAPK	Chemotaxis; immune exclusion; organotropic metastasis	Directed gradients to vessels, BM/LN niches	Plerixafor/other CXCR4 antagonists; timing to preserve hematopoiesis	[69,70]
HGF → MET (growth factor)	CAFs/stroma → MET^+ tumor	RAS/MAPK; PI3K/AKT; STAT3 via GAB1	Collective migration, survival, drug resistance	Enriched at invasive/ vascular fronts	MET inhibitors; consider combos with IO/ECM normalization	[71]
LIF → LIFR (cytokine)	CAFs → tumor	JAK/STAT3	Stemness, EMT state, chemoresistance	PDAC desmoplasia; stromal loops	LIF/LIFR inhibitors with chemotherapy	[72]
IL-11 → IL-11Rα (cytokine)	CAFs (including therapy-stressed) → tumor	JAK/STAT3	Anti-apoptosis (↑BCL-2/ Survivin); EMT; drug resistance	Induced by chemotherapy in CAFs	IL-11/STAT3 targeting to reverse resistance	[73]
CXCL8/IL-8 → CXCR1/2 (chemokine)	CAFs → tumor	SRC→EGFR/ HER2 transactivation; ERK	Invasion, stemness; therapy resistance	Often at inflammatory rims	Anti-CXCL8 mAbs/ CXCR1/2 antagonists in trials	[74]
CCL5 → CCR5 (chemokine)	CAFs/stroma → $CCR5^+$ tumor	NF-κB; PI3K; RHO	Migration/ invasion; DNA-damage response; stemness	High in metastatic niches	CCR5 antagonists (repurposing) under study	[75]
GAS6 → AXL (TAM ligand/RTK)	CAFs/mesenchyme → AXL^+ tumor	PI3K/AKT; MAPK; NF-κB	EMT, invasion, survival	Hypoxic/ invasive fronts	AXL inhibitors (e.g., bemcentinib) combinations	[76]
SEMA3C → NRP1/ITGB1 (axon guidance)	HCC cells↔HSCs/ CAFs (loop)	NF-κB; ↑IL-6; ↑cholesterol biosynthesis	HSC activation; matrix contraction; therapy resistance	HCC stroma; bidirectional feed-forward	Block SEMA3C/ NRP1 or upstream TGF-β	[4]
SEMA4D → PLXNB1 (axon guidance)	Stromal/immune (including CAF/ TAM/osteoclast) → tumor	RHOA/ROCK; PYK2/SRC; c-MET cross-talk	Invasion; angiogenesis; perineural/ osseous remodeling	At invasive and bone niches	Anti-SEMA4D antibodies explored with IO	[77]
SLIT2 → ROBO1 (axon guidance)	CAFs → $ROBO1^+$ tumor	PI3K/AKT/β-catenin (context-dependent)	Context-specific: tumor-suppressive in several settings; prometastatic in others	Often stromal secretion at tumor edge	Axis is bidirectional; consider context before targeting	[78]

(Continued)

Table 2. (Continued)

Axis (class)	Stromal sources → Tumor targets (receptors)	Canonical downstream	Core biological effects	Spatial/ systemic features	Therapeutic notes	Key references
WNT2/WNT5A → FZD/ROR (morphogens)	CAFs → tumor	β-catenin-dependent and noncanonical WNT	Invasion, migration; immune modulation	Peri-tumoral stroma; angiogenic zones	WNT-axis inhibitors; consider toxicity	[79]
JAG1 (Notch ligand) → NOTCH (cell–cell)	CAFs → tumor	NOTCH→HES/ HEY	EMT/stemness; therapy resistance (context-dependent)	Hypoxic/ invasive niches; direct contact	γ-secretase/ Notch-ligand strategies; careful patient selection	[80]
PDGF (growth factor)	CAFs/pericytes → PDGFR^{+} tumor	PI3K/AKT; MAPK	Proliferation, migration; stromal remodeling	Perivascular and fibrotic zones	Multitarget TKIs (context dependent)	[81]
FGF2 → FGFR (growth factor)	CAFs → FGFR^{+} tumor	RAS/MAPK; PI3K/AKT	Proliferation; EMT; resistance	Stromal hubs under stress	FGFR inhibitors (tumor-genotype guided)	[82]
OPN/SPP1 → CD44/integrins (ECM cue)	CAFs/stroma → tumor	FAK/SRC; MAPK; NF-κB	Stemness; migration; immune modulation	Fibrotic rims	Anti-integrin/FAK strategies; biomarker role	[83]
Periostin (POSTN) → αv integrins (ECM cue)	CAFs (PDPN^{+}) → tumor	FAK→YAP/TAZ	Stemness and metastasis programs	Dense desmoplastic stroma	FAK/YAP pathway targeting	[199]
LOX/LOXL (ECM enzyme)	CAFs/hypoxic tumor/ECs → ECM (collagen/ elastin)	Cross-linking enzymes	↑Stiffness/solid stress; perfusion failure; PMN priming	Hypoxic rims; distant premetastatic organs	Pan-LOX inhibition (e.g., PXS-5505) with chemo improves perfusion in PDAC models	[90,91]

TGF-β, transforming growth factor-beta; CAF, cancer-associated fibroblast; TβRI/II, transforming growth factor-beta receptor type I/II; SMAD2/3/4, SMAD family member 2/3/4; PI3K, phosphoinositide 3-kinase; AKT, protein kinase B; MAPK, mitogen-activated protein kinase; EMT, epithelial–mesenchymal transition; MMPs, matrix metalloproteinases; ECM, extracellular matrix; IO, immuno-oncology; IL-6, interleukin-6; IL-6R, interleukin-6 receptor; gp130, glycoprotein 130 (IL6ST); JAK, Janus kinase; STAT3, signal transducer and activator of transcription 3; GSK3β, glycogen synthase kinase-3 beta; EC, endothelial cell; CXCL12, C-X-C motif chemokine ligand 12; SDF-1, stromal cell-derived factor-1; CXCR4, C-X-C chemokine receptor 4; BM, bone marrow; LN, lymph node; FAP, fibroblast activation protein; HGF, hepatocyte growth factor; MET (c-MET), MET proto-oncogene receptor tyrosine kinase; RAS, rat sarcoma (RAS) GTPase; GAB1, GRB2-associated-binding protein 1; LIF, leukemia inhibitory factor; LIFR, leukemia inhibitory factor receptor; IL-11, interleukin-11; IL-11Rα, interleukin-11 receptor alpha; CXCL8 /IL-8, C-X-C motif chemokine ligand 8/interleukin-8; CXCR1, C-X-C chemokine receptor 1; CXCR2, C-X-C chemokine receptor 2; EGFR, epidermal growth factor receptor; HER2, human epidermal growth factor receptor 2 (ERBB2); ERK, extracellular signal-regulated kinase; CCL5, C-C motif chemokine ligand 5; CCR5, C-C chemokine receptor 5; NF-κB, nuclear factor kappa-B; RHO, Ras homolog family (Rho) GTPase; GAS6, growth arrest-specific protein 6; AXL, AXL receptor tyrosine kinase; TAM (receptors), TYRO3–AXL–MERTK receptor tyrosine kinase family; RTK, receptor tyrosine kinase; SEMA3C, semaphorin-3C; NRP1, neuropilin-1; ITGB1, integrin β1; HCC, hepatocellular carcinoma; HSCs, hepatic stellate cells; SEMA4D, semaphorin-4D; PLXNB1, plexin-B1; RHOA, Ras homolog family member A; ROCK, Rho-associated protein kinase; PYK2, proline-rich tyrosine kinase 2 (PTK2B); SRC, proto-oncogene tyrosine-protein kinase Src; SLIT2, slit guidance ligand 2; ROBO1, roundabout guidance receptor 1; β-catenin, beta-catenin; WNT2, Wnt family member 2; WNT5A, Wnt family member 5A; FZD, Frizzled class receptor; ROR, receptor tyrosine kinase-like orphan receptor; CRC, colorectal cancer; GC, gastric cancer; JAG1, Jagged-1; NOTCH, Notch receptor family; HES, Hairy and Enhancer of Split; HEY, Hes-related with YRPW motif; PDGF, platelet-derived growth factor; PDGFR, platelet-derived growth factor receptor; TKIs, tyrosine kinase inhibitors; FGF2, fibroblast growth factor 2; FGFR, fibroblast growth factor receptor; OPN, osteopontin; SPP1, secreted phosphoprotein-1 (gene for osteopontin); CD44, cluster of differentiation 44; FAK, focal adhesion kinase (PTK2); POSTN, periostin; PDPN, podoplanin; αv integrins, integrins containing the alpha-V subunit; YAP, Yes-associated protein; TAZ, transcriptional coactivator with PDZ-binding motif (WWTR1); LOX, lysyl oxidase; LOXL, lysyl oxidase-like protein; PMN, premetastatic niche; PXS-5505, pan-lysyl oxidase inhibitor; PDAC, pancreatic ductal adenocarcinoma

canonical cytokine pathways including TGF-β-induced EMT, JAK/STAT3, and CXCL12/CXCR4 chemotaxis, while recruiting neutrophils to premetastatic niches [106].

Clinically, CAF-derived gene signatures predict metastatic risk and poor survival; recent models in colorectal cancer and oral squamous cell carcinoma demonstrate that CAF-weighted

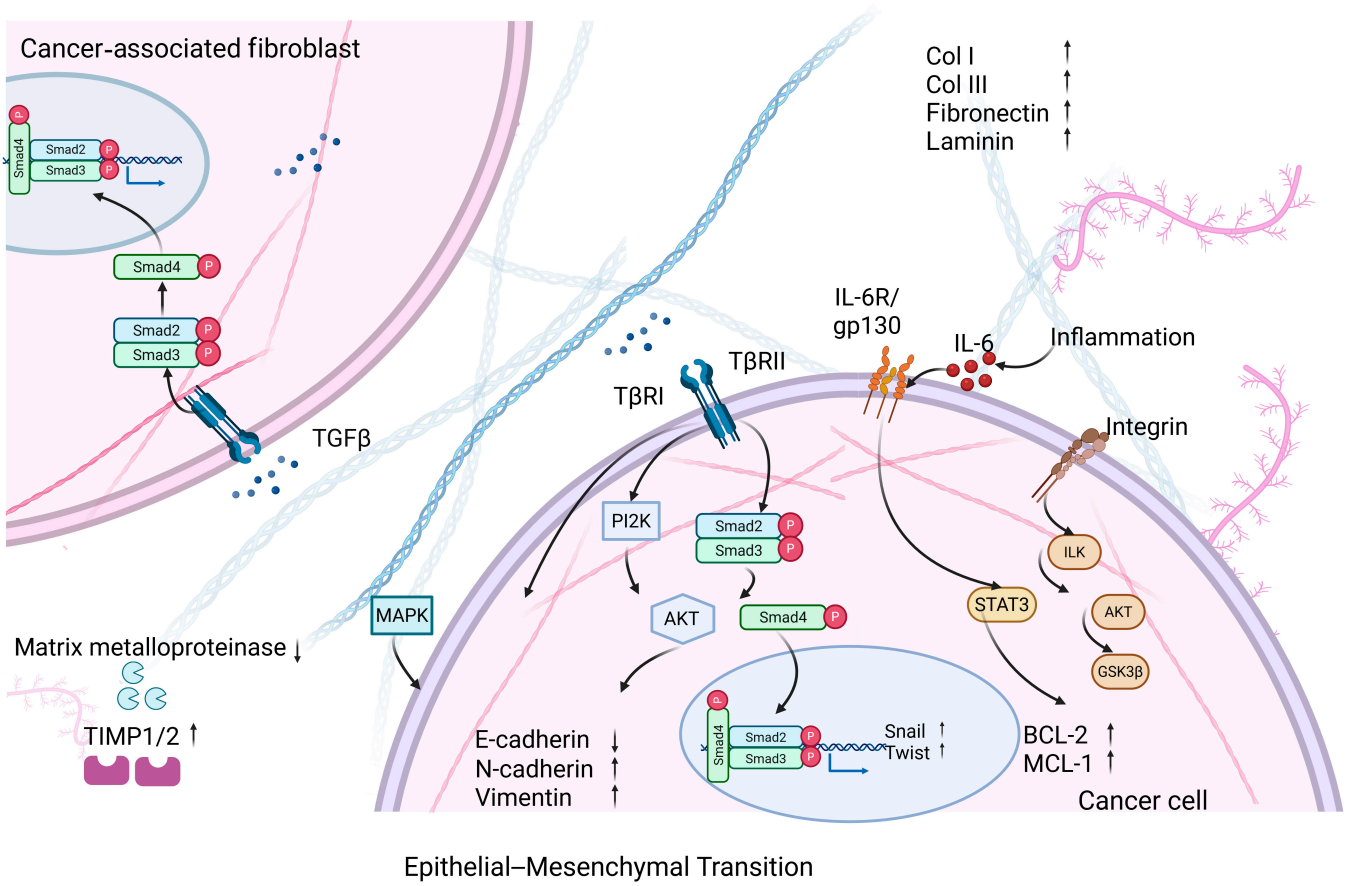


Fig. 4. Cytokine circuits and spatial gradients driving metastasis. Key signaling pathways (TGF-β/SMAD, PI3K/AKT, MAPK, IL-6/STAT3) driven by CAFs activate a prometastatic program in cancer cells. This leads to EMT induction, increased cell survival, and ECM remodeling, collectively facilitating metastasis.

panels or matrix-CAF markers stratify prognosis and align with aggressive disease biology [107].

Clinical Translation of Stromal Cell-Targeted Therapies

Targeting CAFs

Targeting CAFs has become a promising strategy, especially in stromal-rich cancers like PDAC; 2 major approaches are FAP-directed therapies and inhibition of the TGF-β pathway to disrupt protumorigenic CAF functions and recondition the immunosuppressive TME [108].

FAP, overexpressed on CAFs in many epithelial cancers, is being pursued with multiple modalities including antibody–drug conjugates (ADCs); recent platforms use exatecan-class topoisomerase-I payloads and FAP-targeted conjugates or SMDCs to debulk FAP^+ stroma and enable immune engagement, and FAP-targeted radioligand/small-molecule drug conjugate approaches synergize with anti-PD-(L)1 to remodel the TME (increase $CD8^+$/M1 and reduce myeloid-derived suppressor cells [MDSCs]/Tregs) and boost efficacy in preclinical models [109]. FAP-specific cellular therapies are also in early clinical exploration, with reviews summarizing ongoing FAP-CAR (chimeric antigen receptor) programs and broader CAR-T (chimeric antigen receptor T-cell therapy) progress in solid tumors [110]. In parallel, TGF-β inhibition seeks to mitigate CAF-mediated immunosuppression and metastasis. The antisense agent trabedersen (OT-101) targets TGF-β2 and has re-entered clinical testing in combination with pembrolizumab, while contemporary reviews and trials of small-molecule/antibody inhibitors (e.g., vactosertib; discontinued NIS793 program) frame the evolving landscape [111]. Preclinical and early-phase studies indicate that combining TGF-β blockade with cytotoxics can reduce fibroblast activation and tumor burden, consistent with stroma modulation that may improve treatment responses in PDAC [112]. Innovative bifunctional agents that simultaneously neutralize PD-L1 and TGF-β (e.g., SHR-1701, YM101, and the PD-L1/TGF-β bispecific Y101D now in phase 1) enhance T-cell infiltration and M1 polarization in models and have shown early clinical activity, including signals of efficacy in gastrointestinal and pancreatic cancer settings [113].

Anti-angiogenic therapies

CAFs play a key role in therapeutic resistance by up-regulating alternative proangiogenic factors such as fibroblast growth factor (FGF), PDGF, IL-8, and angiopoietins following VEGF inhibition, and by sustaining angiogenesis through cytokine-driven programs [47]. Hypoxia-driven HIF-1α activation further promotes this compensatory angiogenesis, while ECM remodeling by CAFs reduces drug delivery and supports endothelial survival [114].

Resistance also involves the selection of abnormal vascular strategies with reduced VEGF dependence (for example, vessel co-option) and the recruitment of proangiogenic bone-marrow-derived myeloid cells [115]. These adaptations underscore

the necessity for combination strategies [116]. A promising approach combines anti-angiogenic agents with immune checkpoint inhibitors (ICIs) [117]. VEGF inhibition can induce a transient "vascular normalization" window that improves perfusion, reduces hypoxia, and enhances drug penetration and immune-cell infiltration [118]. It also alleviates VEGF-mediated immunosuppression, supporting T-cell function and dendritic-cell maturation [119].

Clinically, the bevacizumab–atezolizumab combination in HCC (IMbrave150) improved overall survival and has emerging translational evidence linking benefit to immune activation (including $CD8^+$ T-cell-related biomarkers), validating this strategy [120]. Optimal outcomes require careful dosing and sequencing, often starting with anti-angiogenic therapy to prime the TME for immunotherapy [121]. Future efforts are focused on multitarget agents, biomarker-guided patient selection, and integrating stromal or metabolic modulators to overcome resistance [122].

Stromal subtype-specific biomarkers

Emerging clinical datasets increasingly support stromal subtype-specific biomarkers as determinants of therapeutic benefit, particularly for immune checkpoint blockade. In metastatic urothelial carcinoma treated with atezolizumab, lack of response was associated with a fibroblast TGF-β signaling signature and an immune-excluded phenotype in which $CD8^+$ T cells are retained in the peritumoral stroma rather than infiltrating tumor nests, highlighting a clinically observable stromal program linked to ICI resistance [123]. In HCC, spatial multiomics defined a tumor immune barrier niche composed of CAFs and $SPP1^+$ macrophages at the tumor boundary that correlates with ICI efficacy, and independent analyses further implicated $POSTN^+$ CAFs as spatial immune response barriers that hinder T-cell infiltration and reduce immunotherapy benefit through an IL-6/STAT3-coupled CAF–macrophage circuit [30]. In colorectal cancer, high-definition spatial mapping showed that the organization of the tumor–stroma boundary stratifies ICI outcomes, where $CXCL14^+$ CAF-rich structural barriers are enriched in nonresponders, whereas ICI-responsive boundaries are characterized by higher abundance and interactions of $LAMP3^+$ DCs and $CXCL13^+$ T cells providing a clinically relevant framework to operationalize stromal niches as response biomarkers [29]. Beyond molecular profiling, low-cost pathology metrics such as tumor–stroma ratio have also been validated as prognostic stromal readouts in colorectal cancer and can serve as a pragmatic companion layer for stratification [124]. Complementing these biomarker advances, several stromal-circuit interventions are being actively tested: for example, the CXCR4 antagonist motixafortide (BL-8040) combined with pembrolizumab and chemotherapy in metastatic PDAC showed immunobiological remodeling (increased intratumoral $CD8^+$ effector T cells and reduced MDSCs) with signals of clinical activity, supporting chemokine-axis targeting as a translatable strategy [125]. FAP-directed approaches are also moving forward, including the FAP-targeted immunocytokine simlukafusp alfa (FAP-IL2v) evaluated in basket-trial settings and combination regimens, and FAP-targeted radioligand therapy such as [^{177}Lu]Lu-FAP-2286 in advanced solid tumors, both reflecting a shift from CAF ablation to targeted delivery and immune reprogramming [126,127].

Importantly, the field has also generated instructive negative results that clarify resistance mechanisms to stroma-targeted therapies. In HA-high metastatic PDAC, the phase III HALO-301 study showed that adding pegvorhyaluronidase alfa (PEGPH20) to nab-paclitaxel/gemcitabine did not improve overall survival, underscoring that single-marker enrichment (HA-high) may be insufficient when stromal programs are dynamic and redundant [128]. Likewise, Hedgehog-pathway inhibition (e.g., vismodegib) failed to improve outcomes in metastatic PDAC, and earlier clinical experience suggested that indiscriminate stromal depletion can yield counterintuitive biology, consistent with stromal plasticity and compensatory rewiring [129]. More broadly, attempts to cotarget stromal cytokine axes such as TGF-β in late-stage trials have not consistently outperformed existing standards (e.g., bintrafusp alfa versus pembrolizumab in PD-L1-high NSCLC), reinforcing that context-dependent pathway dominance and escape via parallel immunosuppressive circuits are common barriers [130].

Challenges in clinical translation

The clinical translation of stromal-targeted therapies is hindered by pronounced stromal heterogeneity and a shortage of validated predictive biomarkers. Recent spatial single-cell atlases show that CAF phenotypes and their neighborhood context vary widely across and within tumors and track with outcome, underscoring the need for context-specific strategies [17]. CAF programs also differ by disease: in PDAC, integrative single-cell and spatial maps detail myofibroblastic, inflammatory, and additional fibroblast clusters that dominate desmoplastic niches, whereas triple-negative breast cancers often harbor inflammatory CAF states that couple angiogenesis with chemoresistance in BRCA1-mutant settings [131]. Beyond this static diversity, CAFs exhibit remarkable plasticity under metabolic and paracrine pressures, with nutrient stress or tumor-derived cues maintaining or reprogramming CAF states and reshaping the microenvironment, mechanisms that can blunt single-agent stromal blockade and favor adaptive resistance [132]. Clinically, these dynamics motivate combination or sequential approaches; for example, concurrent blockade of PD-L1 and TGF-β with SHR-1701, alone or with anti-angiogenic therapy, has shown on-treatment biomarker modulation and early activity in refractory solid tumors, supporting multiaxis targeting of stromal–immune circuits [133]. A central barrier remains the absence of robust, prospectively validated selection tools: although CAF phenotypes and gene programs correlate with prognosis, and vascular "normalization" can be monitored with functional imaging, these readouts have not matured into treatment-guiding biomarkers [17]. Emerging noninvasive stromal imaging is promising, as FAP-targeted positron emission tomography/computed tomography (PET/CT) visualizes fibroblast activation in vivo and is beginning to influence staging and restaging decisions, but prospective trials are still small and heterogeneous [134]. Candidate biophysical markers such as collagen architecture or tissue stiffness are quantifiable by second-harmonic generation microscopy and elastography, yet require standardization and validation for routine use [135]. To overcome these hurdles, platforms that couple organotypic "tumor-microenvironment-on-a-chip" models with multiomics readouts, together with artificial intelligence (AI)-driven biomarker discovery from images and molecular data, are being developed to predict stromal therapy benefit and optimize combinations [136]. Trial designs are adapting as well; basket and platform trials aligned to stromal features, plus window-of-opportunity studies with pharmacodynamic endpoints (for example, first-in-human

anti-TGF-β programs with paired biopsies), can accelerate biomarker qualification and de-risk clinical translation of stromal-targeted regimens [137].

TME Stromal Barrier

Composition and formation of stromal barriers

The stromal barrier is a major obstacle to therapy, integrating mechanical and biochemical impediments that limit transvascular transport and intratumoral diffusion of drugs; recent analyses emphasize dense ECM, elevated interstitial fluid pressure (IFP), and abnormal vasculature as principal determinants of poor delivery [138]. This barrier emerges from continuous, reciprocal signaling between stromal cells and cancer cells that coevolves with disease to create a protective niche favoring progression and treatment resistance [139].

CAFs are central architects of the barrier by overproducing and remodeling ECM macromolecules, particularly fibrillar collagens (types I/III/IV) and hyaluronan, thereby generating a cross-linked, high-density matrix that sterically and hydraulically resists drug penetration [140]. These matrix changes increase stiffness and IFP, further hindering convection and diffusion of therapeutics into tumor parenchyma [141]. Spatially, collagen and hyaluronan accumulate in heterogeneous patterns, with dense peritumoral rims and perivascular niches that correlate with immune exclusion and impaired delivery [140]. CAF activation and ECM deposition are driven by canonical profibrotic pathways, including TGF-β/SMAD, PDGF/PDGFR, and Hedgehog signaling, which are up-regulated across desmoplastic tumors such as PDAC [142].

Tumor vessels exhibit structural and functional abnormalities: endothelial junctional complexes are perturbed (e.g., VE-cadherin and claudin-5 dysregulation), pericyte coverage is reduced or irregular, and basement membranes become discontinuous or abnormally thick, together producing heterogeneous permeability and inefficient, chaotic transport [143]. These aberrations are reinforced by the surrounding matrix and by stromal cross-talk, which destabilize adherens/tight junctions and sustain leakiness and flow heterogeneity [35].

Chronic hypoxia arising from poor perfusion activates HIF-1α programs in fibroblasts and endothelium that increase collagen cross-linking (e.g., LOX/PLOD enzymes), angiogenic signaling, and immunomodulatory ECM remodeling; inflammatory cytokines further sustain CAF activation, creating a self-reinforcing cycle of barrier formation [94].

Multiomics and biophysical studies now link matrix composition/architecture and vascular integrity to drug penetration, motivating combined strategies that normalize ECM mechanics and vessel function (e.g., stiffness/IFP modulation and stromal-targeted delivery) to improve intratumoral exposure [144].

Quantitative evaluation of barrier penetration

Quantitative assessment of stromal-barrier penetration requires pairing advanced imaging with mechanistic modeling to measure, map, and predict drug transport through dense ECM and abnormal vasculature [145]. Multiphoton intravital microscopy (IVM) resolves drug and nanoparticle kinetics, vascular permeability shifts, and cell–cell interactions at single-cell resolution in living tumors, directly revealing spatial heterogeneity of the "enhanced permeability and retention" effect and routes of intravasation/extravasation [146]. Recent IVM syntheses highlight real-time readouts of stromal–immune dynamics relevant to penetration, including endothelial leak, perivascular flow, and immune cell trafficking that condition barrier function [147].

Dynamic contrast-enhanced magnetic resonance imaging provides noninvasive voxelwise estimates of perfusion and permeability. Pharmacokinetic parameters such as the transfer constant K^{trans} and extravascular–extracellular volume fraction V_e quantify size-selective leakage and regional vascular function and have emerging prognostic/response value in oncology [148].

Super-resolution ultrasound surpasses the diffraction limit to depict microvascular networks and flow dynamics inside stromal-dense regions, offering bedside, repeatable microcirculatory readouts of barrier function [149]. Complementary elastography (ultrasound or magnetic resonance) quantifies tumor and peritumoral stiffness, while stiffness gradients correlate with biological behavior and can stratify treatment response [150]. At the nanoscale, super-resolution microscopy (STORM) and expansion-microscopy variants visualize basement-membrane and interstitial ECM architecture (collagen/laminin) that governs pore size and transport resistance [151].

Imaging-informed transport models integrate vascular density, perfusion, interstitial pressure/flow, and drug properties to simulate spatial–temporal distribution and optimize scheduling, for example, sequencing stroma-modulating agents with chemotherapy to exploit transient normalization [152]. Patient-specific, 3D spatiotemporal models built from clinical imaging have been used to simulate radiopharmaceutical delivery and receptor trafficking within tumors, illustrating how image-derived parameters constrain predictions [153]. Broader image-based predictive frameworks and digital-twin/QSP approaches are emerging to personalize PK/PD, link intratumoral concentrations to efficacy, and prospectively test penetration-enhancing strategies in silico [154].

Emerging penetration strategies

Multiomics profiling (single-cell, proteomic, and spatial) has clarified how cytokine-programmed CAF ecosystems propel metastasis and, crucially, where and how stromal barriers should be breached to enable therapeutic delivery. Figure 5 illustrates therapeutic strategies to target stromal components in the TME, encompassing approaches to modify the stromal barrier (e.g., inhibiting ECM remodeling proteases or normalizing aberrant blood vessels); block paracrine signals from CAFs such as connective tissue growth factor (CTGF), HGF, and CXCL12; disrupt cancer cell–ECM interactions mediated by molecules like CXCR4, CD44, or β1-integrins; and directly target CAFs, whether by inhibiting their protumor activity (e.g., via FAPα blockade), delivering therapeutics to CAFs through surface receptors, or reconditioning CAF states (including deactivation, normalization, or immune-mediated eradication). Single-cell studies in melanoma identify metastasis-CAF programs that couple SAA3/IL-1β signaling to neutrophil recruitment, directly linking stromal cytokines to premetastatic niche assembly and suggesting IL-1/IL1RAP blockade as a way to soften stromal defenses [105]. In PDAC, endothelial-like $CD144^+$ (VE-cadherin) CAFs activate β-catenin/STAT3, drive vasculogenic mimicry, and promote dissemination, nominating endoCAF-directed strategies to interrupt pseudo-vascular conduits that impede uniform drug distribution [155]. In OSCC, myCAFs colocalize with tumor cells at the invasive front and up-regulate cancer-cell stemness programs such as CD44, correlating with nodal spread [156].

Mechanistically, cytokine networks organize these barriers and metastatic routes: TGF-β drives EMT transcriptional circuits

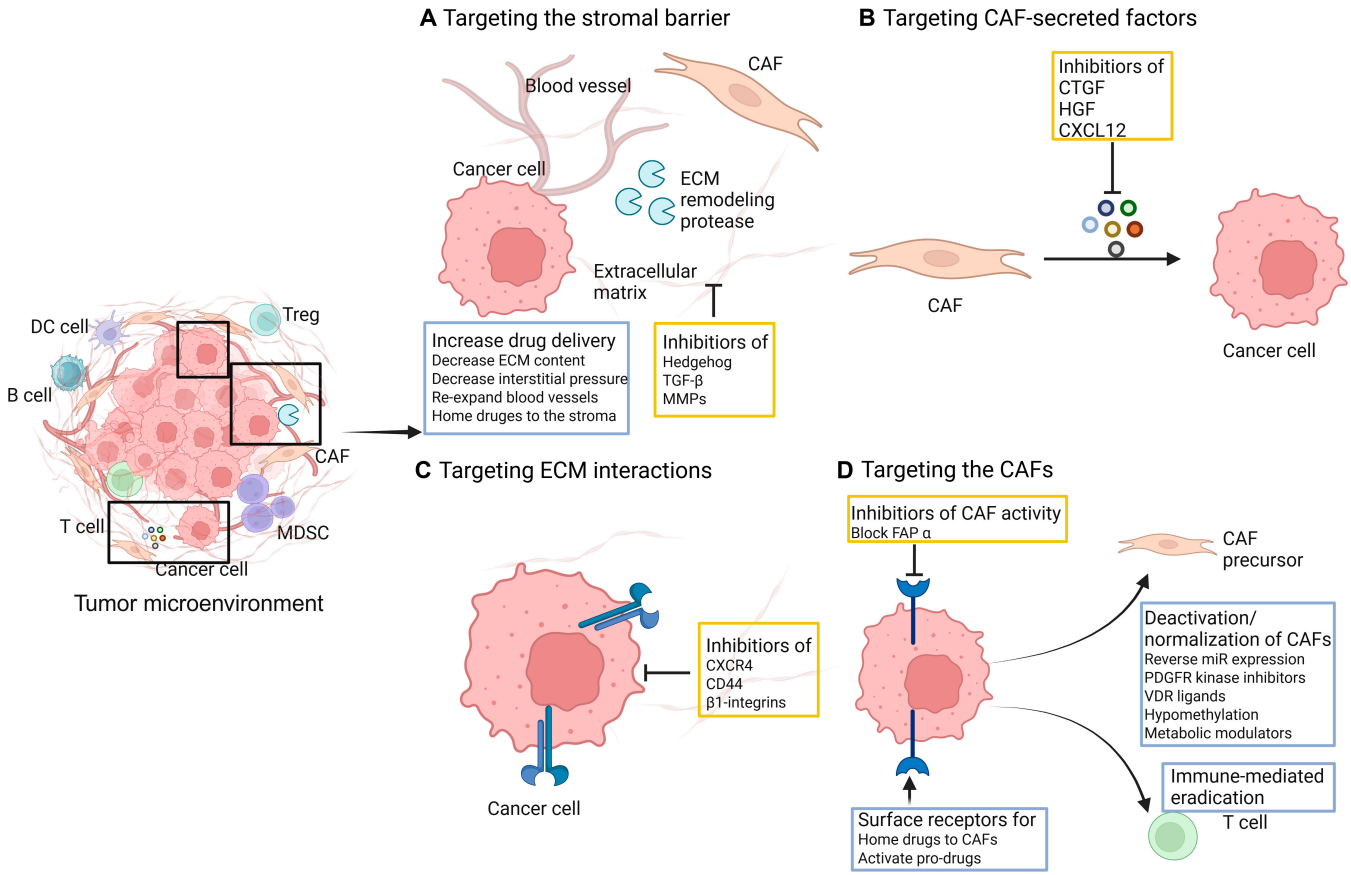


Fig. 5. Strategies for targeting CAF-induced protumorigenic effects. (A) Targeting the stromal barrier modulates ECM remodeling, enhances drug delivery, normalizes vessels, etc., via inhibitors (Hedgehog, TGF-β, and MMPs). (B) Targeting CAF-secreted factors (CTGF, HGF, and CXCL12 inhibitors) disrupts protumor paracrine signaling. (C) Targeting ECM interactions blocks cancer cell receptors (CXCR4, CD44, and β1-integrins). (D) Targeting CAFs involves inhibiting CAF activity (FAPα blockade), drug delivery to CAFs, and CAF deactivation/immune eradication.

(SNAIL/TWIST) and matrix remodeling; IL-6–JAK/STAT3 programs sustain stemness and treatment tolerance; the CXCL12/CXCR4 axis steers tumor-cell homing to stromal sanctuaries; and IL-1β/SAA3 cross-talk enlists myeloid cells to prime premetastatic niches [157]. Clinically oriented stratifiers are emerging: FAP^+ CAFs drive progression and radioresistance in ESCC, and spatially derived 23-gene invasive-front signatures in OSCC predict lymph-node metastasis and survival, actionable readouts to match penetration tactics to stromal topology [158].

These insights directly inform "penetration" strategies that pair barrier mapping with targeted delivery or barrier-loosening. FAP-targeted nanoparticles and radiopharmaceuticals deliver stromal-lytic payloads to FAP-rich regions. Collagenase-decorated nanocarriers or biomaterials temporarily reduce matrix stiffness and improve intratumoral dispersion. CXCR4 antagonists disrupt CXCL12-guided tumor homing to protected niches. CAF-IL1RAP neutralization dampens neutrophil-priming cytokine loops that stiffen the premetastatic niche [159].

Current Challenges and Future Perspectives

Technical challenges

Integrating transcriptomic, epigenomic, proteomic, and spatial modalities is intrinsically difficult because each technology has distinct dynamic ranges, dropout/error structures, and assay-specific biases, which amplify when data are combined; recent reviews and methods papers document that platform heterogeneity and batch effects can obscure stromal signals and hinder subtype discovery if not rigorously addressed [160]. Even within scRNA-seq, droplet (e.g., 10×) and plate-based (e.g., Smart-seq) chemistries differ in sensitivity and noise, and cross-vendor droplet systems vary in capture efficacy and gene-detection capacity, complicating downstream alignment to proteomic or spatial readouts [161].

State-of-the-art batch-correction methods must remove technical variation yet preserve subtle biological gradients that define stromal phenotypes. Mutual nearest-neighbor families (fastMNN/Seurat v5) remain widely used but can distort structure or become order-dependent as batches scale, motivating optimal-transport and semisupervised variants and principled tests of "alignability" before integration [162]. Large benchmarks further show that choices in correction can reshape phenotypes and that evaluation should quantify both batch removal and biology retention across tasks (label transfer, unseen-population detection) [163]. Deep generative models (e.g., scVI/scANVI-style architectures) and new multiomics aligners (e.g., scMODAL) improve vertical and diagonal integration, but require careful tuning and substantial computation, especially for atlas-scale cohorts [164].

A major bottleneck is the absence of standardized, consensus pipelines for stromal cell identification that reconcile discrete "marker lists" with continuous phenotypic spectra. Semisupervised tools for cell-type harmonization across studies (e.g., CellHint)

and population-level learners (e.g., scPoli) help stabilize labels and preserve biological variance during mapping, yet community standards for subtype criteria remain uneven across tissues and diseases [165]. Reference-based integration is emerging as a practical path: Seurat v5 "bridge integration" uses multiome data to align RNA/ATAC and other modalities, while scArches enables federated updating of atlases without raw-data sharing [166]. Spatial data add further complexity (registration, multislice alignment, and cross-platform normalization); recent surveys and algorithms emphasize rigorous validation across sections and instruments [167].

Scalability and accessibility are nontrivial. Atlas-level resources (e.g., HCA and HuBMAP) are pushing standards for data models and sharing, while software ecosystems adopt common containers and file formats, such as SpatialData (scverse) and OME-NGFF (OME-Zarr), to make multimodal spatial images and tables interoperable [168,169]. Visualization and exploration at scale remain challenging; new web frameworks (e.g., Vitessce) aim to render multi-million-cell, multimodal atlases interactively for quality control and hypothesis generation [170].

Looking forward, community benchmarks and curated tumor atlases should serve as reference scaffolds to validate methods and stabilize labels; exemplars include multimodal/diagonal integration benchmarks and learning-based pipelines that map dynamic contrast-enhanced/spatial time series directly to biologically meaningful parameters. Machine learning solutions, multimodal autoencoders for latent cross-modal representations and graph neural networks that encode tissue topology, are particularly promising for stromal biology, provided their outputs are coupled to transparent uncertainty and robust cross-study validation [171].

Biological challenges

Stromal cells, especially CAFs, are highly plastic, toggling between inflammatory iCAF and myofibroblastic myCAF programs under opposing IL-1–JAK/STAT and TGF-β–SMAD cues, with mechanical inputs further biasing state transitions. Such adaptability enables escape from single-axis therapies and fosters treatment resistance [172]. Intercellular cross-talk is multilayered: direct contacts and paracrine ligand–receptor signaling are complemented by CAF-derived extracellular vesicles that reprogram tumor and immune cells, and by tunneling nanotubes that shuttle organelles and metabolites to support invasion and drug tolerance [173]. The functional output of a given pathway (for example, TGF-β between CAFs and cancer cells) depends critically on spatial context, timing, and cellular composition, motivating computational frameworks that integrate single-cell and spatial measurements to infer context-aware communication [174].

Substantial spatial heterogeneity compounds these challenges. i/myCAF mixes and specialized CAF niches differ between invasive fronts, tumor cores, and perivascular hubs that nurture stemness and dissemination; recent spatial atlases in solid tumors (including PDAC and NSCLC) map FAP^+ CAF clusters and $POSTN^+$ CAF neighborhoods linked to immunosuppressive myeloid aggregates [53]. Yet, current single-cell and spatial transcriptomic platforms variably trade sensitivity, resolution, and throughput, and cross-platform integration remains nontrivial, risking loss of subtle stromal gradients without rigorous benchmarking and normalization [175].

Temporal dynamics introduce an additional layer of complexity. Longitudinal single-cell and spatial studies under immunotherapy reveal evolving stromal–immune circuits that correlate with resistance states, yet serial patient sampling is logistically difficult and only partially recapitulated by preclinical models [176]. Progress will hinge on improved lineage tracing to causally track stromal fate transitions (e.g., CRISPR/barcode systems and prime-editing recorders), computational lineage inference from single-cell data, and physiologically faithful stromal–organoid assembloids that enable controlled perturbation [177]. Together, combining high-resolution spatial mapping, causal lineage tools, and mechanistic models of ligand–receptor exchange is essential to decode stromal signaling and plasticity, and to design therapies that anticipate, rather than react to, adaptive resistance [178].

Clinical challenges

Translating stromal biology into clinically useful biomarkers remains difficult because stromal programs are heterogeneous across tumors and evolve with therapy. Unlike relatively stable tumor mutations, stromal phenotypes are plastic and microenvironment-conditioned, myofibroblastic programs dominate desmoplastic PDAC whereas inflammatory CAF states are frequent in basal/TNBC and squamous malignancies, and rCAF subsets can restrain disease, mandating disease-specific validation [131]. Therapy further reshapes stroma: on-treatment single-cell/spatial profiling reveals trajectory switches under immunoradiotherapy, underscoring the need for serial assessment rather than one-time pretreatment stratification [54].

Technical constraints also limit deployment. Routine IHC/RNA assays struggle with overlapping markers, low stromal abundance, and sampling bias from spatial heterogeneity, such as spatial studies that demonstrate block-like regional divergence within single tumors and discordant biomarker status across biopsies [179]. While spatial transcriptomics and multiplexed tissue imaging (e.g., imaging mass cytometry) offer richer readouts, platform variability, FFPE compatibility, and the absence of standardized pipelines continue to impede clinical adoption [180].

Promising measurement strategies are emerging. FAP-PET/CT (e.g., NCT04023240, NCT05262855, and NCT05641896) visualizes fibroblast activation noninvasively and is moving toward procedural standards and early prospective data, enabling whole-body stromal burden mapping for staging and restaging [181,182]. Circulating ECM turnover fragments (e.g., PRO-C3/C3M and related neo-epitopes) quantify desmoplasia and associate with prognosis across cancers, offering scalable, repeatable liquid-biopsy surrogates of stromal activity [183]. CAF-derived extracellular vesicles are increasingly detectable in plasma and carry subtype-linked cargos (miRNAs/proteins) with diagnostic and prognostic utility, though clinical specificity remains to be proven [184]. In parallel, computational pathology can infer stromal states from standard H&E, with deep-learning models imputing transcriptomic programs and predicting outcomes, providing a practical route to deploy stromal signatures at scale [185].

Progress will require large, well-annotated biobanks with serial sampling to capture temporal plasticity; harmonized analysis standards for spatial and multiplex assays; and prospective trials that embed stromal biomarkers into eligibility, stratification, and on-treatment decision rules [186]. Reference-guided integration of multiomics (single-cell plus spatial) can stabilize subtype labels across cohorts, while liquid- and image-based readouts (FAP-PET/CT and ECM fragments) provide repeatable, system-level monitoring, together enabling stromal,

subtype-aware patient selection beyond purely tumor-centric paradigms.

Future directions

Future work should integrate single-cell, spatial multiomics with advanced lineage tracing to resolve stromal origins, plasticity, and fate decisions in situ. Recent advances in CRISPR barcoding, including dual-nuclease Cas9/Cas12a recorders with improved information density, enable linkage of lineage history to cell state at single-cell resolution, while emerging spatiotemporal lineage-tracing frameworks map how clones expand across tissue architecture during tumor growth and metastasis. These tools, coupled with multiomic lineage inference, provide a route to reconstruct developmental trajectories of stromal subpopulations and to pinpoint niche-encoded cues that license protumorigenic functions [187].

Therapeutically, the field should pivot from indiscriminate stromal depletion to precision modulation of pathogenic subtypes while sparing homeostatic stroma. Next-generation effectors include dual-specificity/bispecific ADCs (enhanced avidity and internalization), FAP-directed conjugates/small-molecule drug conjugates for CAF-rich niches, and logic-gated nanotherapies that execute AND-gate delivery or editing only within tumor-conditioned microenvironments. In parallel, epigenetic modulators that reprogram CAF states, such as class I HDAC inhibition curbing myofibroblastic activation in PDAC, or epigenetic payloads delivered by ADCs offer selective rewiring of stromal programs [188,189].

AI-driven stromal subtype prediction models represent a timely future direction for TME research, as they can translate routine imaging into clinically actionable stromal phenotypes for risk stratification and trial design [190,191]. In computational pathology, deep learning can segment tumor epithelium and stroma and compute the tumor–stroma ratio (TSR) automatically, and AI-quantified TSR has shown independent prognostic value across resectable colorectal cancer and pancreatic cancer cohorts [192,193]. Beyond bulk TSR, models that score stromal reaction phenotypes (e.g., fibrosis, cellularity, and orientation at the tumor-stroma interface) enable large-scale, reproducible assessment and can be linked to prognosis-associated molecular signatures [194]. At a higher level of abstraction, imaging-based deep learning has been used to noninvasively classify immune and stroma microenvironment states from CT scans and predict outcomes and treatment benefit, providing a feasible route for longitudinal monitoring of stromal dynamics during therapy [191]. Weakly supervised frameworks such as HistoTME further suggest that WSIs can predict cell type-specific TME signatures (including fibroblast/CAF programs) and immunotherapy response, which could be adapted to output stromal subtype probabilities in clinical workflows [195]. Future multimodal approaches that combine WSI pathomics, radiomics, and spatial transcriptomic supervision may yield interpretable stromal subtype maps to guide patient selection for stroma-targeting or immunomodulatory strategies and to enrich biomarker-driven trials [196].

Multimodal combination strategies should be timed by computational modeling to exploit transient windows of microenvironment "normalization". For matrix-dominated barriers, pan-lysyl-oxidase inhibition (e.g., PXS-5505) reduces collagen cross-linking and improves chemotherapy penetration in preclinical PDAC, while anti-angiogenic dosing can open a short-lived vascular-normalization window that improves perfusion and immunotherapy delivery [90]. Moreover, TME-responsive carriers (pH/MMP-activated) can further concentrate payloads spatiotemporally [197].

Clinical translation will benefit from real-time, biomarker-driven trial designs and adaptive regimens that adjust to on-treatment stromal states, supported by emerging digital-twin and pharmacometric platforms that fuse imaging, spatial-omic, and liquid-biopsy data to prospectively simulate scheduling and combinations [198]. Basket/platform trials anchored to stromal features, coupled with iterative stratification using whole-body stromal imaging and circulating ECM/vesicle readouts, can operationalize stromal reprogramming in routine care [137].

Conclusion

Single-cell and spatial multiomics have transformed stromal biology from a static framework into a dynamic, spatiotemporal system that actively governs tumor progression, immune evasion, drug delivery, and metastatic spread. By resolving conserved stromal archetypes (e.g., myCAFs, iCAFs, endothelial, and pericyte subtypes) and their cytokine circuits (TGF-β, IL-6, and CXCL12/CXCR4), these technologies reveal how ECM architecture, vascular dysfunction, and stromal–immune neighborhoods jointly create therapy-refractory niches. Quantitative imaging and pharmacokinetic modeling now link matrix mechanics and vascular integrity to intratumoral drug exposure, clarifying why monotherapies underperform and why rational combinations, normalizing vessels or matrix while relieving immunosuppression, produce durable benefit only within well-timed therapeutic windows.

Future progress will hinge on integrating lineage-resolved, spatial multiomics with standardizable analytics to decode stromal plasticity in situ and to nominate subtype-specific, low-toxicity interventions. Therapeutically, the field should pivot from broad depletion to precision modulation of pathogenic phenotypes using next-generation modalities, FAP-directed conjugates and radiopharmaceuticals, logic-gated nanotherapies responsive to TME cues, and epigenetic or pathway modulators that reprogram CAF states, embedded within multimodal sequences that first normalize the barrier (e.g., TGF-β or LOX axis modulation and vascular normalization) and then deliver targeted or immune therapies. Clinically, real-time, biomarker-guided and adaptive trial designs, leveraging stromal imaging (e.g., FAP-PET/CT), liquid-biopsy ECM fragments, and computational "digital-twin" scheduling, should enable stromal subtype-aware patient selection and dosing, moving oncology beyond tumor-centric paradigms toward reproducible, spatially precise stromal reprogramming.

Acknowledgments

Funding: The authors declare that they did not receive funding for this work.
Competing interests: The authors declare that they have no competing interests.

References

1. Lavie D, Ben-Shmuel A, Erez N, Scherz-Shouval R. Cancer-associated fibroblasts in the single-cell era. *Nat Cancer*. 2022;3(7):793–807.
2. Liu Y, Sinjab A, Min J, Han G, Paradiso F, Zhang Y, Wang R, Pei G, Dai Y, Liu Y, et al. Conserved spatial subtypes and

cellular neighborhoods of cancer-associated fibroblasts revealed by single-cell spatial multi-omics. *Cancer Cell*. 2025;43(5):905–924.e6.
3. Du K, Jun JH, Dutta RK, Diehl AM. Plasticity, heterogeneity, and multifunctionality of hepatic stellate cells in liver pathophysiology. *Hepatol Commun*. 2024;8(5):Article e0411.
4. Peng H, Yang M, Feng K, Lv Q, Zhang Y. Semaphorin 3C (Sema3C) reshapes stromal microenvironment to promote hepatocellular carcinoma progression. *Signal Transduct Target Ther*. 2024;9(1):Article 169.
5. Obacz J, Valer JA, Nibhani R, Adams TS, Schupp JC, Veale N, Lewis-Wade A, Flint J, Hogan J, Aresu G, et al. Single-cell transcriptomic analysis of human pleura reveals stromal heterogeneity and informs in vitro models of mesothelioma. *Eur Respir J*. 2024;63(1):Article 2300143.
6. Cheng Y, Chen X, Feng L, Yang Z, Xiao L, Xiang B, Wang X, Liu D, Lin P, Shi J, et al. Stromal architecture and fibroblast subpopulations with opposing effects on outcomes in hepatocellular carcinoma. *Cell Discov*. 2025;11(1):Article 1.
7. Glasson Y, Chépeaux LA, Dumé AS, Lafont V, Faget J, Bonnefoy N, Michaud HA. Single-cell high-dimensional imaging mass cytometry: One step beyond in oncology. *Semin Immunopathol*. 2023;45(1):17–28.
8. Severe N, Karabacak NM, Gustafsson K, Baryawno N, Courties G, Kfoury Y, Kokkaliaris KD, Rhee C, Lee D, Scadden EW, et al. Stress-induced changes in bone marrow stromal cell populations revealed through single-cell protein expression mapping. *Cell Stem Cell*. 2019;25(4):570–583.e7.
9. Merens V, Knetemann E, Gürbüz E, De Smet V, Messaoudi N, Reynaert H, Verhulst S, van Grunsven LA. Hepatic stellate cell single cell atlas reveals a highly similar activation process across liver disease aetiologies. *JHEP Rep*. 2025;7(1):Article 101223.
10. Li T, Yang Q, Acs B, Sifakis EG, Toosi H, Engblom C, Thrane K, Lin Q, Mold JE, Sun W, et al. Computational pathology annotation enhances the resolution and interpretation of breast cancer spatial transcriptomics data. *NPJ Precis Oncol*. 2025;9(1):Article 310.
11. van den Brink SC, Sage F, Vértesy Á, Spanjaard B, Peterson-Maduro J, Baron CS, Robin C, Van Oudenaarden A. Single-cell sequencing reveals dissociation-induced gene expression in tissue subpopulations. *Nat Methods*. 2017;14(10):935–936.
12. O'Flanagan CH, Campbell KR, Zhang AW, Kabeer F, Lim JL, Biele J, Eirew P, Lai D, McPherson A, Kong E, et al. Dissociation of solid tumor tissues with cold active protease for single-cell RNA-seq minimizes conserved collagenase-associated stress responses. *Genome Biol*. 2019;20(1):Article 210.
13. Young MD, Behjati S. SoupX removes ambient RNA contamination from droplet-based single-cell RNA sequencing data. *Gigascience*. 2020;9(12):Article giaa151.
14. Cable DM, Murray E, Zou LS, Goeva A, Macosko EZ, Chen F, Irizarry RA. Robust decomposition of cell type mixtures in spatial transcriptomics. *Nat Biotechnol*. 2022;40(4):517–526.
15. Marx V. Method of the year: Spatially resolved transcriptomics. *Nat Methods*. 2021;18(1):9–14.
16. Du Y, Shi J, Wang J, Xun Z, Yu Z, Sun H, Bao R, Zheng J, Li Z, Ye Y. Integration of pan-cancer single-cell and spatial transcriptomics reveals stromal cell features and therapeutic targets in tumor microenvironment. *Cancer Res*. 2024;84(2):192–210.
17. Cords L, Engler S, Haberecker M, Rüschoff JH, Moch H, de Souza N, Bodenmiller B. Cancer-associated fibroblast phenotypes are associated with patient outcome in non-small cell lung cancer. *Cancer Cell*. 2024;42(3):396–412.e5.
18. Mathieson L, Jones P, Koppensteiner L, Neilson L, Dorward DA, O'Connor R, Akram AR. Patient derived cancer-associated fibroblasts from non-small cell lung cancer undergo phenotypic drift in culture. *BJC Rep*. 2025;3(1):Article 50.
19. Felisbino MB, Rubino M, Travers JG, Schuetze KB, Lemieux ME, Anseth KS, Aguado BA, McKinsey TA. Substrate stiffness modulates cardiac fibroblast activation, senescence, and proinflammatory secretory phenotype. *Am J Physiol Heart Circ Physiol*. 2024;326(1):H61–h73.
20. Mitriashkin A, Yap JYY, Fernando EAK, Iyer NG, Grenci G, Fong ELS. Cell confinement by micropatterning induces phenotypic changes in cancer-associated fibroblasts. *Acta Biomater*. 2025;192:61–76.
21. Veghini L, Pasini D, Fang R, Delfino P, Filippini D, Neander C, Vicentini C, Fiorini E, Lupo F, D'Agosto SL, et al. Differential activity of MAPK signalling defines fibroblast subtypes in pancreatic cancer. *Nat Commun*. 2024;15(1):Article 10534.
22. Mucciolo G, Henríquez JA, Jihad M, Teles SP, Manansala JS, Li W, Ashworth S, Lloyd EG, Cheng PS, Luo W, et al. EGFR-activated myofibroblasts promote metastasis of pancreatic cancer. *Cancer Cell*. 2024;42(1):101–118.e11.
23. Semba T, Ishimoto T. Spatial analysis by current multiplexed imaging technologies for the molecular characterisation of cancer tissues. *Br J Cancer*. 2024;131(11):1737–1747.
24. Zheng S, Wang W, Shen L, Yao Y, Xia W, Ni C. Tumor battlefield within inflamed, excluded or desert immune phenotypes: The mechanisms and strategies. *Exp Hematol Oncol*. 2024;13(1):Article 80.
25. Wan Z, Zhang S, Zhong AX, Xu L, Coughlin MF, Pavlou G, Shelton SE, Nguyen HT, Hirose S, Kim S, et al. Transmural flow upregulates PD-L1 expression in microvascular networks. *Adv Sci*. 2024;11(26):Article e2400921.
26. Quintard C, Tubbs E, Jonsson G, Jiao J, Wang J, Werschler N, Laporte C, Pitaval A, Bah TS, Pomeranz G, et al. A microfluidic platform integrating functional vascularized organoids-on-chip. *Nat Commun*. 2024;15(1):Article 1452.
27. Filliol A, Saito Y, Nair A, Dapito DH, Yu LX, Ravichandra A, Bhattacharjee S, Affo S, Fujiwara N, Su H, et al. Opposing roles of hepatic stellate cell subpopulations in hepatocarcinogenesis. *Nature*. 2022;610(7931):356–365.
28. Wang H, Liang Y, Liu Z, et al. $POSTN^{+}$ cancer-associated fibroblasts determine the efficacy of immunotherapy in hepatocellular carcinoma. *J Immunother Cancer*. 2024;12(7):Article e008721.
29. Feng Y, Ma W, Zang Y, Guo Y, Li Y, Zhang Y, Dong X, Liu Y, Zhan X, Pan Z, et al. Spatially organized tumor-stroma boundary determines the efficacy of immunotherapy in colorectal cancer patients. *Nat Commun*. 2024;15(1): Article 10259.
30. Liu Y, Xun Z, Ma K, Liang S, Li X, Zhou S, Sun L, Liu Y, Du Y, Guo X, et al. Identification of a tumour immune barrier in the HCC microenvironment that determines the efficacy of immunotherapy. *J Hepatol*. 2023;78(4):770–782.
31. Öhlund D, Handly-Santana A, Biffi G, Elyada E, Almeida AS, Ponz-Sarvise M, Corbo V, Oni TE, Hearn SA, Lee EJ, et al. Distinct populations of inflammatory fibroblasts and myofibroblasts in pancreatic cancer. *J Exp Med*. 2017;214(3):579–596.

32. Elyada E, Bolisetty M, Laise P, Flynn WF, Courtois ET, Burkhart RA, Teinor JA, Belleau P, Biffi G, Lucito MS, et al. Cross-species single-cell analysis of pancreatic ductal adenocarcinoma reveals antigen-presenting cancer-associated fibroblasts. *Cancer Discov*. 2019;9(8):1102–1123.
33. Cords L, Tietscher S, Anzeneder T, Langwieder C, Rees M, de Souza N, Bodenmiller B. Cancer-associated fibroblast classification in single-cell and spatial proteomics data. *Nat Commun*. 2023;14(1):Article 4294.
34. Yang D, Liu J, Qian H, Zhuang Q. Cancer-associated fibroblasts: From basic science to anticancer therapy. *Exp Mol Med*. 2023;55(7):1322–1332.
35. Augustin HG, Koh GY. A systems view of the vascular endothelium in health and disease. *Cell*. 2024;187(18): 4833–4858.
36. Li J, Wang D, Tang F, Ling X, Zhang W, Zhang Z. Pan-cancer integrative analyses dissect the remodeling of endothelial cells in human cancers. *Natl Sci Rev*. 2024;11(9):Article nwae231.
37. Khan ST, Ahuja N, Taïb S, Vohra S, Cleaver O, Nunes SS. Single-cell meta-analysis uncovers the pancreatic endothelial cell transcriptomic signature and reveals a key role for NKX2-3 in PLVAP expression. *Arterioscler Thromb Vasc Biol*. 2024;44(12):2596–2615.
38. Ribatti D. The role of endothelial junctions in the regulation of the extravasation of tumor cells. A historical reappraisal. *Front Oncol*. 2024;14:1415601.
39. Jimenez-Macias JL, Vaughn-Beaucaire P, Bharati A, Xu Z, Forrest M, Hong J, Sun M, Schmidt A, Clark J, Hawkins W, et al. Modulation of blood-tumor barrier transcriptional programs improves intratumoral drug delivery and potentiates chemotherapy in GBM. *Sci Adv*. 2025;11(9):Article eadr1481.
40. Kane K, Edwards D, Chen J. The influence of endothelial metabolic reprogramming on the tumor microenvironment. *Oncogene*. 2025;44(2):51–63.
41. Dupas A, Goetz JG, Osmani N. Extravasation of immune and tumor cells from an endothelial perspective. *J Cell Sci*. 2024;137(21):Article jcs262066.
42. Hu J, Sa X, Yang Y, Han Y, Wu J, Sun M, Shafi S, Ahmad N, Siraj S, Yang J, et al. Multi-transcriptomics reveals niche-specific expression programs and endothelial cells in glioblastoma. *J Transl Med*. 2025;23(1):Article 444.
43. Xiong K, Pan B, Fang H, Tao Z. Single-cell sequencing analysis reveals cancer-associated pericyte subgroup in esophageal squamous cell carcinoma to predict prognosis. *Front Immunol*. 2024;15:1474673.
44. McErlain T, McCulla EC, Glass MJ, Ziemer LE, Branco CM, Murgai M. Pericytes require physiological oxygen tension to maintain phenotypic fidelity. *Sci Rep*. 2024;14(1): Article 29581.
45. Huang W, Hill JC, Patel S, Richards TD, Sultan I, Kaczorowski DJ, Phillippi JA. Deficiency of fibroblast growth factor 2 promotes contractile phenotype of pericytes in ascending thoracic aortic aneurysm. *Am J Physiol Heart Circ Physiol*. 2025;328(5):H1130–H1143.
46. Du F, Li J, Zhong X, Zhang Z, Zhao Y. Endothelial-to-mesenchymal transition in the tumor microenvironment: Roles of transforming growth factor-β and matrix metalloproteins. *Heliyon*. 2024;10(21):Article e40118.
47. Liu ZL, Chen HH, Zheng LL, Sun LP, Shi L. Angiogenic signaling pathways and anti-angiogenic therapy for cancer. *Signal Transduct Target Ther*. 2023;8(1):Article 198.
48. Paunikar S, Tamagnone L. Connexin-43 in cancer: Above and beyond gap junctions! *Cancer*. 2024;16(24):Article 4191.
49. Xu S, Zhang H, Tian Y. Pericytes in hematogenous metastasis: Mechanistic insights and therapeutic approaches. *Cell Oncol*. 2025;48(4):921–941.
50. Guo T, Xu J. Cancer-associated fibroblasts: A versatile mediator in tumor progression, metastasis, and targeted therapy. *Cancer Metastasis Rev*. 2024;43(3):1095–1116.
51. Jiang Z, Zhou J, Li L, Liao S, He J, Zhou S, Zhou Y. Pericytes in the tumor microenvironment. *Cancer Lett*. 2023;556:Article 216074.
52. Moro M, Balestrero FC, Grolla AA. Pericytes: Jack-of-all-trades in cancer-related inflammation. *Front Pharmacol*. 2024;15:1426033.
53. Croizer H, Mhaidly R, Kieffer Y, Gentric G, Djerroudi L, Leclere R, Pelon F, Robley C, Bohec M, et al. Deciphering the spatial landscape and plasticity of immunosuppressive fibroblasts in breast cancer. *Nat Commun*. 2024;15(1): Article 2806.
54. Shiao SL, Gouin KH, Ing N, Ho A, Basho R, Shah A, Mebane RH, Zitser D, Martinez A, Mevises NY, et al. Single-cell and spatial profiling identify three response trajectories to pembrolizumab and radiation therapy in triple negative breast cancer. *Cancer Cell*. 2024;42(1):70–84.e8.
55. Deng Z, Fan T, Xiao C, Tian H, Zheng Y, Li C, He J. TGF-β signaling in health, disease, and therapeutics. *Signal Transduct Target Ther*. 2024;9(1):Article 61.
56. Tomecka P, Kunachowicz D, Górczyńska J, Gebuza M, Kuźnicki J, Skinderowicz K, Choromańska A. Factors determining epithelial-mesenchymal transition in cancer progression. *Int J Mol Sci*. 2024;25(16):Article 8972.
57. Hirota J, Takeda D, Sadakane Y, Matsuzoe Y, Tadokoro Y, Murakami A, Yatagai N, Saito I, Akashi M, Hasegawa T. TGF-B-induced cancer-associated fibroblast activation promotes tumor progression in oral squamous cell carcinoma mouse model. *Anticancer Res*. 2025;45(9):3687–3700.
58. Garbers C, Aparicio-Siegmund S, Rose-John S. The IL-6/gp130/STAT3 signaling axis: Recent advances towards specific inhibition. *Curr Opin Immunol*. 2015;34:75–82.
59. Reeh H, Rudolph N, Billing U, Christen H, Streif S, Bullinger E, Schliemann-Bullinger M, Findeisen R, Schaper F, Huber HJ, et al. Response to IL-6 trans-and IL-6 classic signalling is determined by the ratio of the IL-6 receptor α to gp130 expression: Fusing experimental insights and dynamic modelling. *Cell Commun Signal*. 2019;17(1):Article 46.
60. Xiong S, Wang R, Chen Q, Luo J, Wang J, Zhao Z, Li Y, Wang Y, Wang X, Cheng B. Cancer-associated fibroblasts promote stem cell-like properties of hepatocellular carcinoma cells through IL-6/STAT3/notch signaling. *Am J Cancer Res*. 2018;8(2):302–316.
61. Chu X, Tian W, Ning J, Xiao G, Zhou Y, Wang Z, Zhai Z, Tanzhu G, Yang J, Zhou R. Cancer stem cells: Advances in knowledge and implications for cancer therapy. *Signal Transduct Target Ther*. 2024;9(1):Article 170.
62. Liu K, Ren T, Huang Y, Sun K, Bao X, Wang S, Zheng B, Guo W. Apatinib promotes autophagy and apoptosis through VEGFR2/STAT3/BCL-2 signaling in osteosarcoma. *Cell Death Dis*. 2017;8(8):Article e3015.
63. Jo MJ, Jeong S, Yun HK, Kim DY, Kim BR, Kim JL, Na YJ, Park SH, Jeong YA, Kim BG, et al. Genipin induces mitochondrial dysfunction and apoptosis via downregulation

of Stat3/mcl-1 pathway in gastric cancer. *BMC Cancer*. 2019;19(1):Article 739.
64. Grivennikov SI, Karin M. Dangerous liaisons: STAT3 and NF-kappaB collaboration and crosstalk in cancer. *Cytokine Growth Factor Rev*. 2010;21(1):11–19.
65. Tian X, Liu F, Wang Z, Zhang J, Liu Q, Zhang Y, Zhang D, Huang C, Zhao J, Jiang S. Modified Biejia Jianwan decoction restrains PD-L1-mediated immune evasion through the HIF-1α/STAT3/NF-κB signaling pathway. *J Ethnopharmacol*. 2024;322:Article 117577.
66. Rose-John S. Local and systemic effects of interleukin-6 (IL-6) in inflammation and cancer. *FEBS Lett*. 2022;596(5): 557–566.
67. Song M, Wang Y, Annex BH, Popel AS. Experiment-based computational model predicts that IL-6 classic and trans-signaling exhibit similar potency in inducing downstream signaling in endothelial cells. *NPJ Syst Biol Appl*. 2023;9(1):Article 45.
68. Rose-John S, Jenkins BJ, Garbers C, Moll JM, Scheller J. Targeting IL-6 trans-signalling: Past, present and future prospects. *Nat Rev Immunol*. 2023;23(10):666–681.
69. Lan H, Wu B, Jin K, Chen Y. Beyond boundaries: Unraveling innovative approaches to combat bone-metastatic cancers. *Front Endocrinol*. 2023;14:1260491.
70. Anastasiadou DP, Quesnel A, Duran CL, Filippou PS, Karagiannis GS. An emerging paradigm of CXCL12 involvement in the metastatic cascade. *Cytokine Growth Factor Rev*. 2024;75:12–30.
71. Pérez-Baena MJ, Cordero-Pérez FJ, Pérez-Losada J, Holgado-Madruga M. The role of GAB1 in cancer. *Cancers (Basel)*. 2023;15(16):Article 4179.
72. Bhatia R, Khan I, Li X, Gautam S, Seshacharyulu P, Alsafwani ZW, Bhyravbhatla N, Ponnusamy MP, Jain M, Malafa M, et al. Targeting cancer-associated fibroblast-driven LIF/LIFR axis improves the therapeutic efficacy of gemcitabine and nab-paclitaxel in pancreatic cancer. *NPJ Precis Oncol*. 2025;9(1):Article 296.
73. Sánchez-Ramírez D, Mendoza-Rodríguez MG, Alemán OR, Candanedo-González FA, Rodríguez-Sosa M, Montesinos-Montesinos JJ, Salcedo M, Brito-Toledo I, Vaca-Paniagua F, Terrazas LI. Impact of STAT-signaling pathway on cancer-associated fibroblasts in colorectal cancer and its role in immunosuppression. *World J Gastrointest Oncol*. 2024;16(5):1705–1724.
74. Lazennec G, Rajarathnam K, Richmond A. CXCR2 chemokine receptor—A master regulator in cancer and physiology. *Trends Mol Med*. 2024;30(1):37–55.
75. Shan J, Xu Y, Lun Y. Comprehensive analysis of the potential biological significance of CCL5 in pan-cancer prognosis and immunotherapy. *Sci Rep*. 2024;14(1):Article 22138.
76. Yadav M, Sharma A, Patne K, Tabasum S, Suryavanshi J, Rawat L, Machaalani M, Eid M, Singh RP, Choueiri TK, et al. AXL signaling in cancer: From molecular insights to targeted therapies. *Signal Transduct Target Ther*. 2025;10(1):Article 37.
77. Fernández-Nogueira P, Linzoain-Agos P, Cueto-Remacha M, De la Guia-Lopez I, Recalde-Percaz L, Parcerisas A, Gascón P, Carbó N, Gutierrez-Uzquiza A, Fuster G, et al. Role of semaphorins, neuropilins and plexins in cancer progression. *Cancer Lett*. 2024;606:Article 217308.
78. Li Q, Zhang XX, Hu LP, Ni B, Li DX, Wang X, Jiang SH, Li H, Yang MW, Jiang YS, et al. Coadaptation fostered by the SLIT2-ROBO1 axis facilitates liver metastasis of pancreatic ductal adenocarcinoma. *Nat Commun*. 2023;14(1): Article 861.
79. Huang TX, Tan XY, Huang HS, Li YT, Liu BL, Liu KS, Chen X, Chen Z, Guan XY, Zou C, et al. Targeting cancer-associated fibroblast-secreted WNT2 restores dendritic cell-mediated antitumour immunity. *Gut*. 2022;71(2):333–344.
80. Shi Q, Xue C, Zeng Y, Yuan X, Chu Q, Jiang S, Wang J, Zhang Y, Zhu D, Li L. Notch signaling pathway in cancer: From mechanistic insights to targeted therapies. *Signal Transduct Target Ther*. 2024;9(1):Article 128.
81. Strell C, Rodríguez-Tomàs E, Östman A. Functional and clinical roles of stromal PDGF receptors in tumor biology. *Cancer Metastasis Rev*. 2024;43(4):1593–1609.
82. Peng M, Deng J, Li X. Clinical advances and challenges in targeting FGF/FGFR signaling in lung cancer. *Mol Cancer*. 2024;23(1):Article 256.
83. Zhao Y, Huang Z, Gao L, Ma H, Chang R. Osteopontin/SPP1: A potential mediator between immune cells and vascular calcification. *Front Immunol*. 2024;15:1395596.
84. Xiao Q, Zhou D, Rucki AA, Williams J, Zhou J, Mo G, Murphy A, Fujiwara K, Kleponis J, Salman B, et al. Cancer-associated fibroblasts in pancreatic cancer are reprogrammed by tumor-induced alterations in genomic DNA methylation. *Cancer Res*. 2016;76(18):5395–5404.
85. Bhagat TD, Von Ahrens D, Dawlaty M, Zou Y, Baddour J, Achreja A, Zhao H, Yang L, Patel B, Kwak C, et al. Lactate-mediated epigenetic reprogramming regulates formation of human pancreatic cancer-associated fibroblasts. *eLife*. 2019;8:Article e50663.
86. Tyan SW, Hsu CH, Peng KL, Chen CC, Kuo WH, Lee EY, Shew JY, Chang KJ, Juan LJ, Lee WH. Breast cancer cells induce stromal fibroblasts to secrete ADAMTS1 for cancer invasion through an epigenetic change. *PLOS ONE*. 2012;7(4):Article e35128.
87. Maeda M, Takeshima H, Iida N, Hattori N, Yamashita S, Moro H, Yasukawa Y, Nishiyama K, Hashimoto T, Sekine S, et al. Cancer cell niche factors secreted from cancer-associated fibroblast by loss of H3K27me3. *Gut*. 2020;69(2):243–251.
88. Yamamoto K, Tateishi K, Kudo Y, Hoshikawa M, Tanaka M, Nakatsuka T, Fujiwara H, Miyabayashi K, Takahashi R, Tanaka Y, et al. Stromal remodeling by the BET bromodomain inhibitor JQ1 suppresses the progression of human pancreatic cancer. *Oncotarget*. 2016;7(38): 61469–61484.
89. Becker WR, Nevins SA, Chen DC, Chiu R, Horning AM, Guha TK, Laquindanum R, Mills M, Chaib H, Ladabaum U, et al. Single-cell analyses define a continuum of cell state and composition changes in the malignant transformation of polyps to colorectal cancer. *Nat Genet*. 2022;54(7):985–995.
90. Chitty JL, Yam M, Perryman L, Parker AL, Skhinas JN, Setargew YF, Mok ET, Tran E, Grant RD, Latham SL, et al. A first-in-class pan-lysyl oxidase inhibitor impairs stromal remodeling and enhances gemcitabine response and survival in pancreatic cancer. *Nat Cancer*. 2023;4(9):1326–1344.
91. Patras L, Shaashua L, Matei I, Lyden D. Immune determinants of the pre-metastatic niche. *Cancer Cell*. 2023;41(3):546–572.
92. Wang Y, Jia J, Wang F, Fang Y, Yang Y, Zhou Q, Yuan W, Gu X, Hu J, Yang S. Pre-metastatic niche: Formation, characteristics and therapeutic implication. *Signal Transduct Target Ther*. 2024;9(1):Article 236.

93. Chen MM, Gao Q, Ning H, Chen K, Gao Y, Yu M, Liu CQ, Zhou W, Pan J, Wei L, et al. Integrated single-cell and spatial transcriptomics uncover distinct cellular subtypes involved in neural invasion in pancreatic cancer. *Cancer Cell*. 2025;43(9):1656–1676.e10.
94. Mai Z, Lin Y, Lin P, Zhao X, Cui L. Modulating extracellular matrix stiffness: A strategic approach to boost cancer immunotherapy. *Cell Death Dis*. 2024;15(5):Article 307.
95. Liao J, Chen R, Lin B, Deng R, Liang Y, Zeng J, Ma S, Qiu X. Cross-talk between the TGF-β and cell adhesion signaling pathways in cancer. *Int J Med Sci*. 2024;21(7):1307–1320.
96. Hu Y, Dong Z, Liu K. Unraveling the complexity of STAT3 in cancer: Molecular understanding and drug discovery. *J Exp Clin Cancer Res*. 2024;43(1):Article 23.
97. Wang MJ, Zhang HL, Chen F, Guo XJ, Liu QG, Hou J. The double-edged effects of IL-6 in liver regeneration, aging, inflammation, and diseases. *Exp Hematol Oncol*. 2024;13(1):Article 62.
98. Zarrer J, Taipaleenmäki H. The osteoblast in regulation of tumor cell dormancy and bone metastasis. *J Bone Oncol*. 2024;45:Article 100597.
99. Allgayer H, Mahapatra S, Mishra B, Swain B, Saha S, Khanra S, Kumari K, Panda VK, Malhotra D, Patil NS, et al. Epithelial-to-mesenchymal transition (EMT) and cancer metastasis: The status quo of methods and experimental models 2025. *Mol Cancer*. 2025;24(1):Article 167.
100. Shi X, Wang X, Yao W, Shi D, Shao X, Lu Z, Chai Y, Song J, Tang W, Wang X. Mechanism insights and therapeutic intervention of tumor metastasis: Latest developments and perspectives. *Signal Transduct Target Ther*. 2024;9(1): Article 192.
101. Zhou M, Wang J, Pan J, Wang H, Huang L, Hou B, Lai Y, Wang F, Guan Q, Wang F, et al. Nanovesicles loaded with a TGF-β receptor 1 inhibitor overcome immune resistance to potentiate cancer immunotherapy. *Nat Commun*. 2023;14(1):Article 3593.
102. Håkansson L, Dunér P, Broströmer E, Gustavsson B, Wettergren Y, Ghafouri B, Håkansson A, Clinchy B. A new IL-6-inducing mechanism in cancer with new therapeutic possibilities. *Cancer*. 2024;16(21):Article 3588.
103. Yang Y, Li J, Lei W, Wang H, Ni Y, Liu Y, Yan H, Tian Y, Wang Z, Yang Z, et al. CXCL12-CXCR4/CXCR7 axis in cancer: From mechanisms to clinical applications. *Int J Biol Sci*. 2023;19(11):3341–3359.
104. Forsthuber A, Aschenbrenner B, Korosec A, Jacob T, Annusver K, Krajic N, Kholodniuk D, Frech S, Zhu S, Purkhauser K, et al. Cancer-associated fibroblast subtypes modulate the tumor-immune microenvironment and are associated with skin cancer malignancy. *Nat Commun*. 2024;15(1):Article 9678.
105. Tauch S, Hey J, Kast B, Gengenbacher N, Weiß L, Sator-Schmitt M, Lohr S, Brobeil A, Schirmacher P, Utikal J, et al. A unique signature for cancer-associated fibroblasts in melanoma metastases. *Pigment Cell Melanoma Res*. 2025;38(2):Article e70002.
106. Jin W, Yu Q, Yu L, Zhou T, Wang X, Lu W, Zhang X, Ding L, Hu Q, Ni Y. HAS1^{high} cancer associated fibroblasts located at the tumor invasion front zone promote oral squamous cell carcinoma invasion via ECM remodeling. *J Exp Clin Cancer Res*. 2025;44(1):Article 238.
107. Liang C, Ji D, Qin F, Chen G. CAF signature predicts the prognosis of colorectal cancer patients: A retrospective study based on bulk RNA sequencing and single-cell RNA sequencing data. *Medicine*. 2023;102(10):Article e33149.
108. Finan JM, Guo Y, Goodyear SM, Brody JR. Challenges and opportunities in targeting the complex pancreatic tumor microenvironment. *JCO Oncol Adv*. 2024;1:Article e2400050.
109. Weng W, Meng T, Zhao Q, Shen Y, Fu G, Shi J, Zhang Y, Wang Z, Wang M, Pan R, et al. Antibody-exatecan conjugates with a novel self-immolative moiety overcome resistance in colon and lung cancer. *Cancer Discov*. 2023;13(4):950–973.
110. Meng S, Hara T, Miura Y, Ishii H. Fibroblast activation protein constitutes a novel target of chimeric antigen receptor T-cell therapy in solid tumors. *Cancer Sci*. 2024;115(11):3532–3542.
111. D'Cruz OJ, Qazi S, Hwang L, Ng K, Trieu V. Impact of targeting transforming growth factor β-2 with antisense OT-101 on the cytokine and chemokine profile in patients with advanced pancreatic cancer. *Onco Targets Ther*. 2018;11:2779–2796.
112. Qiang L, Hoffman MT, Ali LR, Castillo JI, Kageler L, Temesgen A, Lenehan P, Wang SJ, Bello E, Cardot-Ruffino V, et al. Transforming growth factor-β blockade in pancreatic cancer enhances sensitivity to combination chemotherapy. *Gastroenterology*. 2023;165(4):874–890.e10.
113. Zhang H, Chen J, Bai J, Zhang J, Huang S, Zeng L, Zhou P, Shen Q, Yin T. Single dual-specific anti-PD-L1/TGF-β antibody synergizes with chemotherapy as neoadjuvant treatment for pancreatic ductal adenocarcinoma: A preclinical experimental study. *Int J Surg*. 2024;110(5):2679–2691.
114. Patel SA, Nilsson MB, Le X, Cascone T, Jain RK, Heymach JV. Molecular mechanisms and future implications of VEGF/VEGFR in cancer therapy. *Clin Cancer Res*. 2023;29(1):30–39.
115. Cannell IG, Sawicka K, Pearsall I, Wild SA, Deighton L, Pearsall SM, Lerda G, Joud F, Khan S, Bruna A, et al. FOXC2 promotes vasculogenic mimicry and resistance to anti-angiogenic therapy. *Cell Rep*. 2023;42(8):Article 112791.
116. Sherafat NS, Keshavarz A, Mardi A, Mohammadiara A, Aghaei M, Aghebati-Maleki L, Mohammadi MH. Rationale of using immune checkpoint inhibitors (ICIs) and anti-angiogenic agents in cancer treatment from a molecular perspective. *Clin Exp Med*. 2025;25(1):Article 238.
117. Li Y, Yang L, Liu Z. Combination of immune checkpoint inhibitors and anti-angiogenic agents: An emerging strategy for cancer therapy. *Crit Rev Oncol Hematol*. 2025;215: Article 104883.
118. Mpekris F, Panagi M, Charalambous A, Voutouri C, Stylianopoulos T. Modulating cancer mechanopathology to restore vascular function and enhance immunotherapy. *Cell Rep Med*. 2024;5(7):Article 101626.
119. Kang Y, Li H, Liu Y, Li Z. Regulation of VEGF-A expression and VEGF-A-targeted therapy in malignant tumors. *J Cancer Res Clin Oncol*. 2024;150(5):Article 221.
120. Kudo M, Finn RS, Galle PR, Zhu AX, Ducreux M, Cheng AL, Ikeda M, Tsuchiya K, Aoki KI, Jia J, et al. IMbrave150: Efficacy and safety of atezolizumab plus bevacizumab versus sorafenib in patients with Barcelona clinic liver cancer stage B unresectable hepatocellular carcinoma: An exploratory analysis of the phase III study. *Liver Cancer*. 2023;12(3):238–250.
121. Xu Q, Shao D. Leveraging the synergy between anti-angiogenic therapy and immune checkpoint inhibitors to treat digestive system cancers. *Front Immunol*. 2024;15:1487610.

122. Yang S, Fang Y, Ma Y, Wang F, Wang Y, Jia J, Yang Y, Sun W, Zhou Q, Li Z. Angiogenesis and targeted therapy in the tumour microenvironment: From basic to clinical practice. *Clin Transl Med*. 2025;15(4):Article e70313.
123. Mariathasan S, Turley SJ, Nickles D, Castiglioni A, Yuen K, Wang Y, Kadel Iii EE, Koeppen H, Astarita JL, Cubas R, et al. TGFβ attenuates tumour response to PD-L1 blockade by contributing to exclusion of T cells. *Nature*. 2018;554(7693):544–548.
124. Huijbers A, Tollenaar RA, v Pelt GW, Zeestraten EC, Dutton S, McConkey CC, Domingo E, Smit VT, Midgley R, Warren BF, et al. The proportion of tumor-stroma as a strong prognosticator for stage II and III colon cancer patients: Validation in the VICTOR trial. *Ann Oncol*. 2013;24(1): 179–185.
125. Bockorny B, Semenisty V, Macarulla T, Borazanci E, Wolpin BM, Stemmer SM, Golan T, Geva R, Borad MJ, Pedersen KS, et al. BL-8040, a CXCR4 antagonist, in combination with pembrolizumab and chemotherapy for pancreatic cancer: The COMBAT trial. *Nat Med*. 2020;26(6):878–885.
126. Li L, Ding H, Chen L, Zheng W, Zhang Y, Chen Y. Initial results and clinical experiences of [^{177}Lu]Lu-FAP-2286 for pleural metastases: A single-center retrospective study. *J Nucl Med*. 2026.
127. Liu W, Zhang N, Zheng W, et al. Comparative evaluation of [^{68}Ga]Ga-FAP-2286 and [^{18}F]FDG PET/CT in breast cancer and initial experience with [^{177}Lu]Lu-FAP-2286 therapy. *Eur J Nucl Med Mol Imaging*. 2026.
128. Van Cutsem E, Tempero MA, Sigal D, Oh DY, Fazio N, Macarulla T, Hitre E, Hammel P, Hendifar AE, Bates SE, et al. Randomized phase III trial of pegvorhyaluronidase alfa with nab-paclitaxel plus gemcitabine for patients with hyaluronan-high metastatic pancreatic adenocarcinoma. *J Clin Oncol*. 2020;38(27):3185–3194.
129. Catenacci DV, Junttila MR, Karrison T, Bahary N, Horiba MN, Nattam SR, Marsh R, Wallace J, Kozloff M, Rajdev L, et al. Randomized phase Ib/II study of gemcitabine plus placebo or vismodegib, a hedgehog pathway inhibitor, in patients with metastatic pancreatic cancer. *J Clin Oncol*. 2015;33(36):4284–4292.
130. Cho BC, Lee JS, Wu YL, Cicin I, Dols MC, Ahn MJ, Cuppens K, Veillon R, Nadal E, Dias JM, et al. Bintrafusp alfa versus pembrolizumab in patients with treatment-naive, programmed death-ligand 1-high advanced NSCLC: A randomized, open-label, phase 3 trial. *J Thorac Oncol*. 2023;18(12):1731–1742.
131. Kim S, Leem G, Choi J, Koh Y, Lee S, Nam SH, Kim JS, Park CH, Hwang HK, Min KI, et al. Integrative analysis of spatial and single-cell transcriptome data from human pancreatic cancer reveals an intermediate cancer cell population associated with poor prognosis. *Genome Med*. 2024;16(1):Article 20.
132. Zhang Y, Ling L, Murad R, Maganti S, Manceau A, Hetrick HA, Neff M, Galapate CM, Grenier SF, Carrette F, et al. Macropinocytosis maintains CAF subtype identity under metabolic stress in pancreatic cancer. *Cancer Cell*. 2025;43(9):1677–1696.e15.
133. Yi L, Pan H, Ning Z, Xu L, Zhang H, Peng L, Liu Y, Yang Y, Si W, Wang Y, et al. Clinical and biomarker analyses of SHR-1701 combined with famitinib in patients with previously treated advanced biliary tract cancer or pancreatic ductal adenocarcinoma: A phase II trial. *Signal Transduct Target Ther*. 2024;9(1):Article 347.
134. Mori Y, Dendl K, Cardinale J, Kratochwil C, Giesel FL, Haberkorn U. FAPI PET: Fibroblast activation protein inhibitor use in oncologic and nononcologic disease. *Radiology*. 2023;306(2):Article e220749.
135. Chen X, Chen L, Miao J, Huang X, Han X, Zheng L, Xu S, Chen J, Li L. Prognostic significance of collagen signatures in pancreatic ductal adenocarcinoma obtained from second-harmonic generation imaging. *BMC Cancer*. 2024;24(1):Article 652.
136. Ravi K, Zhang Y, Sakala L, Manoharan TJ, Pockaj B, LaBaer J, Park JG, Nikkhah M. Tumor microenvironment on-a-chip and single-cell analysis reveal synergistic stromal-immune crosstalk on breast cancer progression. *Adv Sci*. 2025;12(16):Article e2413457.
137. Duan XP, Qin BD, Jiao XD, Liu K, Wang Z, Zang YS. New clinical trial design in precision medicine: Discovery, development and direction. *Signal Transduct Target Ther*. 2024;9(1):57.
138. Li X, Hu Y, Zhang X, Shi X, Parak WJ, Pich A. Transvascular transport of nanocarriers for tumor delivery. *Nat Commun*. 2024;15(1):Article 8172.
139. Liao T, Chen X, Qiu F, Zhang X, Wu F, Zhao Z, Xu M, Chen M, Shen JW, Shen Q, et al. Regulation of cancer-associated fibroblasts for enhanced cancer immunotherapy using advanced functional nanomedicines: An updated review. *J Nanobiotechnology*. 2025;23(1):166.
140. Yuan Z, Li Y, Zhang S, Wang X, Dou H, Yu X, Zhang Z, Yang S, Xiao M. Extracellular matrix remodeling in tumor progression and immune escape: From mechanisms to treatments. *Mol Cancer*. 2023;22(1):48.
141. Zhang M, Zhang B. Extracellular matrix stiffness: Mechanisms in tumor progression and therapeutic potential in cancer. *Exp Hematol Oncol*. 2025;14(1):54.
142. Giarratana AO, Prendergast CM, Salvatore MM, Capaccione KM. TGF-β signaling: Critical nexus of fibrogenesis and cancer. *J Transl Med*. 2024;22(1):594.
143. Delgado-Bellido D, Oliver FJ, Vargas Padilla MV, Lobo-Selma L, Chacón-Barrado A, Díaz-Martin J, de Álava E. VE-cadherin in cancer-associated angiogenesis: A deceptive strategy of blood vessel formation. *Int J Mol Sci*. 2023;24(11):Article 9343.
144. He X, Yang Y, Han Y, Cao C, Zhang Z, Li L, Xiao C, Guo H, Wang L, Han L, et al. Extracellular matrix physical properties govern the diffusion of nanoparticles in tumor microenvironment. *Proc Natl Acad Sci USA*. 2023;120(1):Article e2209260120.
145. Cassani M, Fernandes S, Pagliari S, Cavalieri F, Caruso F, Forte G. Unraveling the role of the tumor extracellular matrix to inform nanoparticle design for nanomedicine. *Adv Sci*. 2025;12(2):Article e2409898.
146. Fernandez JL, Snipstad S, Bjørkøy A, Davies CL. Real-time multiphoton intravital microscopy of drug extravasation in tumours during acoustic cluster therapy. *Cells*. 2024;13(4):Article 349.
147. Hirao H, Honda M, Tomita M, Li L, Adawy A, Xue W, Hibi T. Intravital imaging of immune responses in the cancer microenvironment. *Cancer Med*. 2025;14(8):Article e70899.
148. Wang D, Liu S, Fu J, Zhang P, Zheng S, Qiu B, Liu H, Ye Y, Guo J, Zhou Y, et al. Correlation of K(trans) derived from dynamic contrast-enhanced MRI with treatment

response and survival in locally advanced NSCLC patients undergoing induction immunochemotherapy and concurrent chemoradiotherapy. *J Immunother Cancer*. 2024;12(6):Article e008574.
149. Hoyt K. Super-resolution ultrasound imaging for monitoring the therapeutic efficacy of a vascular disrupting agent in an animal model of breast cancer. *J Ultrasound Med*. 2024;43(6):1099–1107.
150. Kwon MR, Youn I, Ko ES, Choi SH. Correlation of shear-wave elastography stiffness and apparent diffusion coefficient values with tumor characteristics in breast cancer. *Sci Rep*. 2024;14(1):7180.
151. Bharadwaj A, Kumar A, Mathew SP, Mitra R, Bhattacharyya J, Jaganathan BG, Boruah BR. Advancing cellular insights: Super-resolution STORM imaging of cytoskeletal structures in human stem and cancer cells. *Biochem Biophys Rep*. 2024;39:Article 101798.
152. Moradi Kashkooli F, Kolios MC. Multi-scale and multi-physics models of the transport of therapeutic/diagnostic cancer agents. *Cancer*. 2023;15(24):Article 5850.
153. Piranfar A, Moradi Kashkooli F, Zhan W, Bhandari A, Saboury B, Rahmim A, Soltani M. Radiopharmaceutical transport in solid tumors via a 3-dimensional image-based spatiotemporal model. *NPJ Syst Biol Appl*. 2024;10(1):39.
154. Bhandari A, Gu B, Kashkooli FM, Zhan W. Image-based predictive modelling frameworks for personalised drug delivery in cancer therapy. *J Control Release*. 2024;370:721–746.
155. Sun X, Cai W, Li H, Gao C, Ma X, Guo Y, Fu D, Xiao D, Zhang Z, Wang Y, et al. Endothelial-like cancer-associated fibroblasts facilitate pancreatic cancer metastasis via vasculogenic mimicry and paracrine signalling. *Gut*. 2025;74(9):1437–1451.
156. Furudate K, Kasai S, Yoshizawa T, Sasaki Y, Fujikura K, Goto S, Ito R, Takagi K, Tanaka T, Kijima H, et al. Spatial colocalization and molecular crosstalk of myofibroblastic CAFs and tumor cells shape lymph node metastasis in oral squamous cell carcinoma. *PLOS Genet*. 2025;21(9):Article e1011791.
157. Gottumukkala SB, Ganesan TS, Palanisamy A. Comprehensive molecular interaction map of TGFβ induced epithelial to mesenchymal transition in breast cancer. *NPJ Syst Biol Appl*. 2024;10(1):Article 53.
158. Zhou X, Tong Y, Yu C, Pu J, Zhu W, Zhou Y, Wang Y, Xiong Y, Sun X. FAP positive cancer-associated fibroblasts promote tumor progression and radioresistance in esophageal squamous cell carcinoma by transferring exosomal lncRNA AFAP1-AS1. *Mol Carcinog*. 2024;63(10):1922–1937.
159. Abbasi S, Khademi S, Montazerabadi A, Sahebkar A. FAP-targeted nanoparticle-based imaging in cancer: A systematic review. *J Biomed Phys Eng*. 2024;14(4):323–334.
160. Lv T, Zhang Y, Liu J, Kang Q, Liu L. Multi-omics integration for both single-cell and spatially resolved data based on dual-path graph attention auto-encoder. *Brief Bioinform*. 2024;25(5):Article bbae450.
161. Gezelius H, Enblad AP, Lundmark A, Åberg M, Blom K, Rudfeldt J, Raine A, Harila A, Rendo V, Heinäniemi M, et al. Comparison of high-throughput single-cell RNA-seq methods for ex vivo drug screening. *NAR Genom Bioinform*. 2024;6(1):Article lqae001.
162. Yu X, Xu X, Zhang J, Li X. Batch alignment of single-cell transcriptomics data using deep metric learning. *Nat Commun*. 2023;14(1):960.
163. Arevalo J, Su E, Ewald JD, van Dijk R, Carpenter AE, Singh S. Evaluating batch correction methods for image-based cell profiling. *Nat Commun*. 2024;15(1):Article 6516.
164. Ge S, Sun S, Xu H, Cheng Q, Ren Z. Deep learning in single-cell and spatial transcriptomics data analysis: Advances and challenges from a data science perspective. *Brief Bioinform*. 2025;26(2):Article bbaf136.
165. Xu C, Prete M, Webb S, Jardine L, Stewart BJ, Hoo R, He P, Meyer KB, Teichmann SA. Automatic cell-type harmonization and integration across human cell atlas datasets. *Cell*. 2023;186(26):5876–5891.e20.
166. Hao Y, Stuart T, Kowalski MH, Choudhary S, Hoffman P, Hartman A, Srivastava A, Molla G, Madad S, Fernandez-Granda C, et al. Dictionary learning for integrative, multimodal and scalable single-cell analysis. *Nat Biotechnol*. 2024;42(2):293–304.
167. Khan M, Arslanturk S, Draghici S. A comprehensive review of spatial transcriptomics data alignment and integration. *Nucleic Acids Res*. 2025;53(12):Article gkaf536.
168. Li T, Horsfall D, Basurto-Lozada D, Roberts K, Prete M, Lawrence JE, He P, Tuck E, Moore J, Yoldas AK, et al. WebAtlas pipeline for integrated single-cell and spatial transcriptomic data. *Nat Methods*. 2025;22(1):3–5.
169. Marconato L, Palla G, Yamauchi KA, Virshup I, Heidari E, Treis T, Vierdag WM, Toth M, Stockhaus S, Shrestha RB, et al. SpatialData: An open and universal data framework for spatial omics. *Nat Methods*. 2025;22(1):58–62.
170. Keller MS, Gold I, McCallum C, Manz T, Kharchenko PV, Gehlenborg N. Vitessce: Integrative visualization of multimodal and spatially resolved single-cell data. *Nat Methods*. 2025;22(1):63–67.
171. Liu T, Fang ZY, Zhang Z, Yu Y, Li M, Yin MZ. A comprehensive overview of graph neural network-based approaches to clustering for spatial transcriptomics. *Comput Struct Biotechnol J*. 2024;23:106–128.
172. Melchionna R, Trono P, Di Carlo A, Di Modugno F, Nisticò P. Transcription factors in fibroblast plasticity and CAF heterogeneity. *J Exp Clin Cancer Res*. 2023;42(1):Article 347.
173. Su J, Song Y, Zhu Z, Huang X, Fan J, Qiao J, Mao F. Cell-cell communication: New insights and clinical implications. *Signal Transduct Target Ther*. 2024;9(1):Article 196.
174. Dimitrov D, Schäfer PS, Farr E, Rodriguez-Mier P, Lobentanzer S, Badia-i-Mompel P, Dugourd A, Tanevski J, Ramirez Flores RO, Saez-Rodriguez J. LIANA+ provides an all-in-one framework for cell-cell communication inference. *Nat Cell Biol*. 2024;26(9):1613–1622.
175. Janesick A, Shelansky R, Gottscho AD, Wagner F, Williams SR, Rouault M, Beliakoff G, Morrison CA, Oliveira MF, Sicherman JT, et al. High resolution mapping of the tumor microenvironment using integrated single-cell, spatial and in situ analysis. *Nat Commun*. 2023;14(1):Article 8353.
176. Chen Y, Wang D, Li Y, Qi L, Si W, Bo Y, Chen X, Ye Z, Fan H, Liu B, et al. Spatiotemporal single-cell analysis decodes cellular dynamics underlying different responses to immunotherapy in colorectal cancer. *Cancer Cell*. 2024;42(7):1268–1285.e7.
177. Zhang X, Huang Y, Yang Y, Wang QE, Li L. Advancements in prospective single-cell lineage barcoding and their applications in research. *Genome Res*. 2024;34(12):2147–2162.
178. Gong D, Arbesfeld-Qiu JM, Perrault E, Bae JW, Hwang WL. Spatial oncology: Translating contextual biology to the clinic. *Cancer Cell*. 2024;42(10):1653–1675.

179. Liu X, Zhang K, Kaya NA, Jia Z, Wu D, Chen T, Liu Z, Zhu S, Hillmer AM, Wuestefeld T, et al. Tumor phylogeography reveals block-shaped spatial heterogeneity and the mode of evolution in hepatocellular carcinoma. *Nat Commun*. 2024;15(1):3169.
180. Pang JM, Byrne DJ, Bergin AR, Caramia F, Loi S, Gorringe KL, Fox SB. Spatial transcriptomics and the anatomical pathologist: Molecular meets morphology. *Histopathology*. 2024;84(4):577–586.
181. Hope TA, Calais J, Goenka AH, Haberkorn U, Konijnenberg M, McConathy J, Oprea-Lager DE, Trimnal L, Zan E, Herrmann K, et al. SNMMI procedure standard/EANM practice guideline for fibroblast activation protein (FAP) PET. *J Nucl Med*. 2025;66(1):26–33.
182. Karbhari A, Mosessian S, Trivedi KH, Valla F Jr, Jacobson M, Truty MJ, Patnam NG, Simeone DM, Zan E, Brennan T, et al. Gallium-68-labeled fibroblast activation protein inhibitor-46 PET in patients with resectable or borderline resectable pancreatic ductal adenocarcinoma: A phase 2, multicenter, single arm, open label non-randomized study protocol. *PLOS ONE*. 2023;18(11):Article e0294564.
183. Fan Y, Moser J, van Meurs M, Kiers D, Sand JM, Leeming DJ, Pickkers P, Burgess JK, Kox M, Pillay J. Neo-epitope detection identifies extracellular matrix turnover in systemic inflammation and sepsis: An exploratory study. *Crit Care*. 2024;28(1):120.
184. Gou Z, Li J, Liu J, Yang N. The hidden messengers: Cancer associated fibroblasts-derived exosomal miRNAs as key regulators of cancer malignancy. *Front Cell Dev Biol*. 2024;12:1378302.
185. Hoang DT, Dinstag G, Shulman ED, Hermida LC, Ben-Zvi DS, Elis E, Caley K, Sammut SJ, Sinha S, Sinha N, et al. A deep-learning framework to predict cancer treatment response from histopathology images through imputed transcriptomics. *Nat Cancer*. 2024;5(9):1305–1317.
186. Bollhagen A, Bodenmiller B. Highly multiplexed tissue imaging in precision oncology and translational cancer research. *Cancer Discov*. 2024;14(11):2071–2088.
187. Chen C, Liao Y, Zhu M, Wang L, Yu X, Li M, Peng G. Dual-nuclease single-cell lineage tracing by Cas9 and Cas12a. *Cell Rep*. 2025;44(1):Article 115105.
188. Gu Y, Wang Z, Wang Y. Bispecific antibody drug conjugates: Making 1+1>2. *Acta Pharm Sin B*. 2024;14(5):1965–1986.
189. Liang G, Oh TG, Hah N, Tiriac H, Shi Y, Truitt ML, Antal CE, Atkins AR, Li Y, Fraser C, et al. Inhibiting stromal class I HDACs curbs pancreatic cancer progression. *Nat Commun*. 2023;14(1):Article 7791.
190. Koike Y, Aokage K, Ikeda K, Nakai T, Tane K, Miyoshi T, Sugano M, Kojima M, Fujii S, Kuwata T, et al. Machine learning-based histological classification that predicts recurrence of peripheral lung squamous cell carcinoma. *Lung Cancer*. 2020;147:252–258.
191. Jiang Y, Zhang Z, Wang W, Huang W, Chen C, Xi S, Ahmad MU, Ren Y, Sang S, Xie J, et al. Biology-guided deep learning predicts prognosis and cancer immunotherapy response. *Nat Commun*. 2023;14(1):Article 5135.
192. Zhao K, Li Z, Yao S, Wang Y, Wu X, Xu Z, Wu L, Huang Y, Liang C, Liu Z. Artificial intelligence quantified tumour-stroma ratio is an independent predictor for overall survival in resectable colorectal cancer. *EBioMedicine*. 2020;61:Article 103054.
193. Vendittelli P, Bokhorst JM, Smeets EM, Kryklyva V, Brosens LA, Verbeke C, Litjens G. Automatic quantification of tumor-stroma ratio as a prognostic marker for pancreatic cancer. *PLOS ONE*. 2024;19(5):Article e0301969.
194. Jiang J, Tekin B, Yuan L, Armasu S, Winham SJ, Goode EL, Liu H, Huang Y, Guo R, Wang C. Computational tumor stroma reaction evaluation led to novel prognosis-associated fibrosis and molecular signature discoveries in high-grade serous ovarian carcinoma. *Front Med*. 2022;9:Article 994467.
195. Patkar S, Chen A, Basnet A, Bixby A, Rajendran R, Chernet R, Faso S, Kumar PA, Desai D, El-Zammar O, et al. Predicting the tumor microenvironment composition and immunotherapy response in non-small cell lung cancer from digital histopathology images. *NPJ Precis Oncol*. 2024;8(1):Article 280.
196. Kim JY, Jeong H, Valero Puche A, Song S, Cho SI, Jung M. Artificial intelligence-driven quantification of tumor-stroma ratio and fibroblasts enables precise classification of stroma quality and quantity in predicting colorectal cancer recurrence. *Pathobiology*. 2025;92(5):276–287.
197. Sun H, Li Y, Xue M, Feng D. Tumor microenvironment-responsive nanoparticles: Promising cancer PTT carriers. *Int J Nanomedicine*. 2025;20:7987–8001.
198. Ștefănigă SA, Cordoș AA, Ivascu T, Feier CV, Muntean C, Stupinean CV, Călinici T, Aluaș M, Bolboacă SD. Advancing precision oncology with digital and virtual twins: A scoping review. *Cancer*. 2024;16(22):Article 3817.
199. Miyako S, Koma YI, Nakanishi T, Tsukamoto S, Yamanaka K, Ishihara N, Azumi Y, Urakami S, Shimizu M, Kodama T, et al. Periostin in cancer-associated fibroblasts promotes esophageal squamous cell carcinoma progression by enhancing cancer and stromal cell migration. *Am J Pathol*. 2024;194(5):828–848.